University of Nevada, Reno

Towards Developing a Scanning Position Sensitive Detector (PSD) Microscopy: PSD Measurement Enhancement, Adaptive Local Scanning and Implementation

A thesis submitted in partial fulfillment of the
requirements for the degree of Master of Science
in Electrical Engineering

by

Seyed Mehdi Rahimi

Dr. Yantao Shen, Thesis Advisor

August, 2016

THE GRADUATE SCHOOL

We recommend that the thesis
prepared under our supervision by

SEYED MEHDI RAHIMI

Entitled

Towards Developing a Scanning Position Sensitive Detector (PSD) Microscopy: PSD Measurement Enhancement, Adaptive Local Scanning and Implementation

be accepted in partial fulfillment of the
requirements for the degree of

MASTER OF SCIENCE

Yantao Shen, Ph.D., Advisor

Hao Xu, Ph.D., Committee Member

Hung La, Ph.D., Graduate School Representative

David W. Zeh, Ph.D., Dean, Graduate School

August, 2016

Abstract

A Position Sensitive Detector/Device (PSD) is a sensor that is capable of tracking the location of a laser beam on its surface. PSDs are used in many scientific instruments and technical applications including but not limited to: Atomic-force microscopy (AFM), human eye movement monitoring, mirrors or machine tool alignment, vibration analysis, beam position control and so on. This work intends to propose a new application using the PSD. That is a new microscopy system called scanning PSD microscopy. The working mechanism is about putting an object on the surface of the PSD and fast scanning its area with a laser beam. To achieve a high degree of accuracy and precision, a reliable framework was designed using the PSD. In this work, we first tried to improve the PSD reading and its measurement performance. This was done by minimizing the effects of noise, distortion and other disturbing parameters. After achieving a high degree of confidence, the microscopy system can be implemented based on the improved PSD measurement performance. Later to improve the scanning efficiency, we developed an adaptive local scanning system to scan the whole area of the PSD in a short matter of time. It was validated that our comprehensive and adaptive local scanning method can shorten the scanning time in order of hundreds of times in comparison to the traditional raster scanning without losing any important information about the scanned 2D objects. This developed method, would allow to scan the surface of the PSD by using square-shaped blocks of light instead of a single point of the laser beam. Methods are also introduced to scan very complicated objects with bifurcations and crossings. By incorporating all these methods, the new microscopy system is capable of scanning very complicated objects in the matter of a few seconds with a resolution that is in order of a few micrometers.

Acknowledgments

I would like to thank my committee members Dr. Yantao Shen, Dr. Hao Xu and Dr. Hung La. I would like to give additional thanks to Dr. Yantao Shen, who has allowed me to work in his Lab for the last three years and has provided a great deal of guidance, support and assistance in my pursuit to complete my thesis and graduate study at the University of Nevada, Reno. I would also like to thank my fellow grad students Yudong Luo and Abhijaat Sidher for ideas and feedbacks that have been absolutely invaluable.

Dedication

I would like to dedicate this thesis to my wife, Farzaneh Chalyavi
for all of her love and support.

Contents

List of Tables

List of Figures

Chapter 1

Introduction

A Position Sensitive Device (PSD) is a sensor that is capable of tracking laser beam on its surface. The four current outputs of the sensor would give the position of the light incident. In this work, we have used some of the PSD characteristics to develop a new kind of microscopy system. Using this system, a user can put a small object (something that is even as small as a few micrometers) on the surface of the PSD and then by using the system, she can get the dimensions of the objects with a very good accuracy and precision.

To achieve this, we first had to improve the accuracy of the PSD. Chapter 2 talks about how we did this improvement. A PSD sensor can be affected by numerous factors including noise, distortion, rotation, vibration and etc. The first part of this work addresses these challenges. All of the noises that are affecting the system are analyzed one by one and preventive measures have been taken to lessen their effect as much as possible. The distortion problem of the PSD is also discussed in this chapter. A method is used to rectify the distortion effect of the PSD. Various validations have been done to make sure that the effect of noise and distortion is mitigated. Other challenges such as X-Y mismatch and rotation correction is also discussed in this chapter. At the end and based on the new improved PSD system, a microscopy system is proposed. The system works in this manner that a user can put an object on the surface of the PSD and by scanning the area of the PSD, one can find the object and its dimensions.

In chapter 3, we continue to improve the microscopy system by developing and

implementing an adaptive local scanning for the PSD. Although a traditional scanning (or raster scanning) needs to scan every pixel of an area to find the object on the surface of the PSD, we suggested an adaptive local scanning to minimizing the time needed for this scanning. This is done by first using an initial scanning which would roughly find the position of the object and then a fine scanning that uses a sinusoidal pattern to scan the boundaries of the object. The pattern would follow the curvature of the object and would even recognize bifurcations and crossings. This smart algorithm would change the amplitude and frequency of the sine wave automatically to match the circumstances of the object. A very sophisticated algorithm would use an Archimedean spiral to find missed points of the curve and to recognize all the crossings and bifurcations. Eventually, the algorithm would scan the whole object no matter how many branches or crossings it has. The algorithm even has a sub-routine for thick objects that would fit in the sinusoidal pattern and therefore can scan these objects much faster than by going around them. At the end, a Fourier curve fitting is employed to get even better results from the reading we got from the scanning pattern. Extensive implementation results demonstrated that the fitting can reduce the scanning error to an almost half of the original value. It also validates that our comprehensive and adaptive local scanning method can shorten the scanning time in order of hundreds of times in comparison to the traditional raster scanning without losing any important information about the scanned object.

Based on the previous works, in chapter 4, we took a new approach to making the scanning even faster. In this approach, instead of using a single point of laser for scanning the PSD, we used square-shaped blocks of light to locate the object in a few shots. This would eliminate the limitations of the micromanipulator and can decrease the scanning time significantly. In the previous approach, a laser was required to move to scan the PSD area, the scanning speed would be directly dependent on the speed of the movement of the micromanipulator. No matter how much we increase the speed of the motors, there would still be this problem of moving the laser beam from one side to another. In this new approach, a projector, focused on the PSD, would act like

the laser beam and would give illumination on any points at any time. Since the only delay would be the refresh rate of the projector, which is in the scale of kilohertz, the scanning point can jump to any position in a time that is much faster than what PSD can capture. A Digital Light Processing (DLP) was used to give the best performance as the projector. Then we developed a new algorithm similar to the Quadtree method which in fact would follow a 2D bisection algorithm to find the object very quickly. This approach is to substitute the initial scanning that we had before. This would increase the scanning time significantly since the only limitation in time would be the response time of the PSD.

By putting all these methods together, we can have a microscopy system that can scan and find the dimensions of a very small object in the matter of a few seconds with a very high accuracy and precision.

1.1 Organization of Thesis

This thesis has been prepared based on three papers. Each paper covers a portion of study as explained in the previous section. The papers were converted to the same style of the other parts of the thesis. For more information and to get the electronic print link, contact the author at mrahimi@unr.edu. The title, a short summary and publication status of each paper (at the time of thesis submission) are described below:

Title: Improving Measurement Accuracy of Position Sensitive Detector (PSD) for a New Scanning PSD Microscopy System

Short summary: This paper described the important steps used in the calibration and validation of the Position Sensitive Detector (PSD). PSD can be greatly affected by inaccuracies in interface circuits, system connections, outside environmental changes and the semi-conductive properties of the sensor. The presence of these factors causes noises and distortions that heavily degrade the performance of the PSD and any system built on it. This work addresses improving measurement accuracy of the PSD by using various correcting methods and filters to eliminate signal noises throughout the system and also develops a distortion rectifying methodology to rectify

pincushion-type radial distortion associated with the PSD devices. The improved PSD system can be further used for a proposed scanning PSD microscopy system. The system is capable of scanning an object and finding its dimensions in the scale of a few micrometers.

Publication status: Published in Robotics and Biomimetics (ROBIO), 2014 IEEE International Conference on Pages 1685 - 1690

Citation: *Mehdi Rahimi, Yudong Luo, Frederick C. Harris, Sergiu M. Dascalu, and Yantao Shen. "Improving measurement accuracy of Position Sensitive Detector (PSD) for a new scanning PSD microscopy system." In Robotics and Biomimetics (ROBIO), 2014 IEEE International Conference on, pp. 1685-1690. IEEE, 2014. http://dx.doi.org/10.1109/ROBIO.2014.7090577*

Title: Adaptive Local Scanning: A Comprehensive and Intelligent Method for Fast Scanning of Indiscrete Objects

Short summary: This paper addresses one of the challenges of scanning the whole area of the PSD. Usually, a pixel-by-pixel scanning which is called raster scanning is used to scan the area of the PSD but this approach can be time-consuming. This work presents an adaptive local scanning method for efficiently sampling indiscrete objects such as string-like one-piece connected objects under the microscopy. An initial scanning pattern is firstly investigated. Once the initial scanning reaches the object, an adaptive sinusoidal scanning method that can on-line adjust its scanning frequency and amplitude by predicting both the curvatures and the shape of the object is then developed and applied. The method also addresses scanning intersections and bifurcations associated with objects. Based on extensive implementation, it was validated that this method can be much faster and more efficient than traditional scanning. This approach would help the proposed PSD Microscopy to scan an object in a very short amount of time.

Publication status: Published in Intelligent Robots and Systems (IROS), 2015 IEEE/RSJ International Conference on Pages 4955 - 4960

Citation: *Mehdi Rahimi, and Yantao Shen. "Adaptive local scanning: A*

comprehensive and intelligent method for fast scanning of indiscrete objects." In Intelligent Robots and Systems (IROS), 2015 IEEE/RSJ International Conference on, pp. 4955-4960. IEEE, 2015. http://dx.doi.org/10.1109/IROS.2015.7354074

Title: Accelerated Adaptive Local Scanning of Complicated Micro Objects for the PSD Scanning Microscopy: Methods and Implementation

Short summary: In previous works, a PSD-based microscopy was introduced to scan sophisticated objects using the PSD sensor and a laser beam connected to an X-Y table. Although promising results were obtained from that system, the speed of the scanning was still dependent on the speed of the movement of the micromanipulator. This work presents an extension to the tracing method and also introduces a completely novel system to eliminate the limitations of the micromanipulator. The simulations show a very fast scanning that does not need a laser and can scan the whole area of the PSD in a very short time. Putting this method alongside the previous work we can get to a PSD Microscopy that can scan the dimension of an object in a matter of few seconds.

Publication status: Under review for possible publication in the 14th International Conference on Intelligent Autonomous Systems (IAS-14)

Citation: *Mehdi Rahimi, and Yantao Shen. "Accelerated Adaptive Local Scanning of Complicated Micro Objects for the PSD Scanning Microscopy: Methods and Implementation" In International Conference on Intelligent Autonomous Systems (IAS-14) 2016. (under review).*

Chapter 2

Improving Measurement Accuracy of Position Sensitive Detector (PSD) for a New Scanning PSD Microscopy System

2.1 Abstract

The measurement accuracy of Position Sensitive Detector (PSD) can be greatly affected by inaccuracies in interface circuits, system connections, outside environmental changes and the semi-conductive properties of the sensor. The presence of these factors causes noises and distortions that heavily degrade the performance of the PSD and any system built on it. This work addresses improving measurement accuracy of the PSD by using various correcting methods and filters to eliminate signal noises throughout the system and also develops a distortion rectifying methodology to rectify pincushion-type radial distortion associated with the PSD devices, which would enhance measurement accuracy in a larger active area of the PSD. Experimental validation demonstrates the effectiveness of these accuracy improvement methods. The improved PSD system can be further used for a proposed scanning PSD microscopy system. The system is capable of scanning an object in the scale of a few micrometers for rapidly measuring the dimensions of the object based on the vanishing effect and the multi-channel photocurrent feedback mechanism. Preliminary results show the measurement performance of the proposed microscopy.

2.2 Introduction

A Position Sensitive Detector/Device (PSD) is a sensor capable of tracking the location of a laser beam on its surface. A PSD basically consists of a uniform resistive layer formed on one or both surfaces of a high-resistivity semiconductor substrate and a pair of electrodes formed on both ends of the resistive layer for extracting position signals. The active area, which is also a resistive layer, has a P-N junction that generates photocurrent by means of the photovoltaic effect. PSDs can track very small positional changes of laser spot over the active area and directly output the position data with high resolution, high-speed response and high reliability [1]. There are two major types of PSDs available: Lateral PSDs and Segmented PSDs. In this work, we focus on using a two-dimensional Lateral PSD. Lateral effect PSDs are continuous single element planar diffused photodiodes with no gaps or dead areas [2]. The factors that degrade the measurement accuracy of all types of PSDs generally include: (1) the aberration of the optical system, (2) the size of the light spot, (3) the position detection error of a PSD device and its resolution, (4) the dark current and environment stray light, (5) the accuracy and noise of the PSD detection circuit, (6) the temperature drift of the electronic circuit and optical system, (7) the tilting of the surface being measured, (8) the unevenness of the surface being measured, (9) the X-Y mismatch of the electrodes, (10) the difference of reflective characteristics of the surface being measured and (11) the distortions caused by the integration process of the PSD chip and its interface circuit. These factors strongly affect the position resolution and accuracy of a PSD system and are usually hard to be fully removed during the implementation of the PSD systems [1][3]. Position resolution of a PSD can be defined as the minimum displacement that can be resolved by its sensing elements, while accuracy is the closeness of its position output to the actual laser beam position in a given electro-optical system. These are important properties of the sensing system as they characterize the quality of the sensing response of the system for smaller signals or displacements. The presence of noise and degradation heavily

hampers the signal-to-noise ratio.

To improve the measurement accuracy of a lateral-effect PSD system, in this work, different noises are identified, analyzed, and eliminated by the signal averaging. In addition, effects of X-Y mismatch and rotations are corrected. Finally, a distortion rectifying algorithm effectively solving pincushion-type radial distortions is developed. Both simulation and experimental results verify the effectiveness of the developed accuracy improvement methods. Such a PSD system with high reliability and accuracy can be further used for a proposed scanning PSD microscopy. The microscopy is based on the vanishing effect and the multi-channel photo- current feedback mechanism of the PSD. The vanishing effect is related to the four zero or low photocurrent outputs when the laser beam is blocked by meeting the object on the PSD surface. Several methods for detecting the exact positions where the blockings of the laser occur are proposed and implemented. Once the blocking positions of a scanning laser beam pattern are determined, the 2-D dimension of the micro-object on the PSD surface can be accurately measured. Preliminary results on accurately and rapidly measuring both opaque and transparent objects demonstrate the performance of the proposed microscopy system.

The paper is structured as follows: In section 2.3, the lateral effect PSD is introduced and some of its main properties are discussed. Section 2.4 is structured into four parts that describe our methods used to improve the accuracy of PSD, including a discussion about noises affecting the system and the used filtering method, the X-Y mismatch and rotation correction, the pincushion type distortion and the proposed rectifying method, and mapping results. A new scanning PSD microscopy is discussed in detail in section 2.5. The vanishing effect and the multi-channel photocurrent feedback mechanism are covered and preliminary experiment and results show the performance of the proposed microscopy.

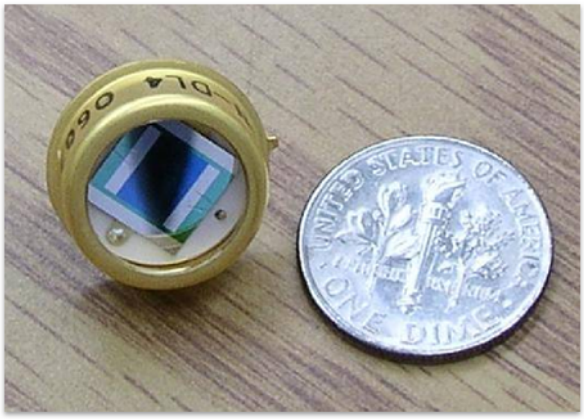

Figure 2.1: Photograph of lateral effect PSD chip.

2.3 The Lateral Effect PSD

To implement our improvement methods, we have chosen a Duo-lateral effect PSD (OSI Optoelectronics DL-4S) for building up the testbed and modeling. The lateral effect PSD is shown in Fig. 2.1 is a 2-D sensor with $4mm \times 4mm$ active area. In a lateral effect PSD, the relative two-dimensional position of light beams such as a laser beam on the active surface of the chip can be expressed as:

$$\begin{aligned} X &= \frac{I_{x1} - I_{x2}}{I_{x1} + I_x 2} \\ Y &= \frac{I_{y1} - I_{y2}}{I_{y1} + I_{y2}} \end{aligned} \tag{2.1}$$

Where X represents the relative position of the laser spot on the X-axis and Y is the relative position on the Y-axis. Also I_{x1} , I_{x2} , I_{y1} , I_{y2} are photo currents measured in the direction indicated by the index, which in the following experiments are called Channel A, B, C and D respectively.

A very important property that has been used several times in the following experiments is that because of the structure of the PSD, opposite channels have inverse

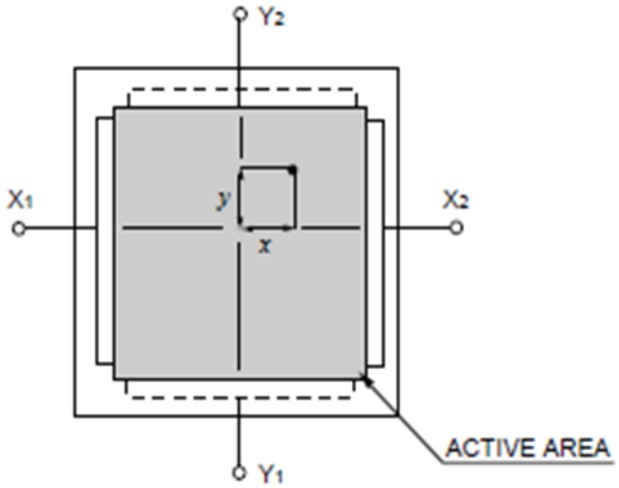

Figure 2.2: Schematic illustration showing the two electrodes are mounted on opposite sides of the PSD to determine X-axis and Y-axis direction.

correlation; meaning that when one of them increases, the other one decreases. This effect can be easily seen in Fig. 2.2.

The major advantage of the lateral type PSD is that the accuracy of the output is not affected by the laser spot profile or its intensity distribution. The positional resolution of about $0.5\mu m$ is sufficient for positioning in micro-level. Another outstanding property of this type is the position linearity over relatively large areas of the active surface of the chip. This is important for our task since it allows us to keep errors at a low level during filtering, rectifying, and mapping processes. The signal conditioning circuit of the PSD can be employed and found in [4].

2.4 Accuracy Improvement Methods And Experimental Validation

2.4.1 Noises and Filtering

There are different sources of noise for the whole system. The micro-manipulator motor that controls the laser, the ambient light on the PSD, the PSD board and its

connections, the amplifiers, the probe, the dSPACE panel and control board -which is used to get the data from the PSD board- and finally any movements in the area that may cause the PSD or the laser to shake. Luckily, this work was set up on an anti-vibration table that was able to absorb movement noises to some acceptable degree but there were still lots of other noises. A set of tests were designed and run to measure each of these noises and their impact on the system. The dSPACE noise is the most negligible noise as it produces a noise that results in less than $1\mu m$ movement in each direction which is shown in Fig. 2.3-(a). This noise is probably because of the dSPACE internal oscillator crystal. Another test measures the noise that the dSPACE and the PSD produce together but without any laser beam, meaning that it just shows the effect of ambient light and the noise of the PSD board. This is can be seen in Fig. 2.3- (b). We also noticed that the micro-manipulator motor that moves the laser has a considerable noise. This can be seen when comparing Fig. 2.3-(c) and Fig. 2.3-(d). And finally, the noise that the whole system produces when everything is on and working can be seen in Fig. 2.3-(d). Notice that in all of these experiments, the motor is not receiving any command to move so the noise of the system is causing a vibration as high as almost $1\mu m$ in each direction. Note that all the figures in Fig. 2.3 have been centered for easier comparison.

Fast Fourier Transform (FFT), can be used as a powerful tool for analyzing and measuring noise signals as we can effectively measure the frequency content. Unfortunately, the only problem for this system is that, as it can be seen in Fig. 2.4, the noise does not occur in any special frequency. In another word, the system has a noise that is more similar to white noise. This means that the low-pass filters, band-pass filters, or similar approaches are not applicable for filtering out the noise of this system. But as in this experiment, the DC part of the signal is more important to us, we can use other methods to eliminate the noise. One can just use an AC to DC converter but that would remove useful information too.

Signal averaging is a signal processing technique applied in the time domain, intended to increase the strength of a signal relative to noise that is obscuring it.

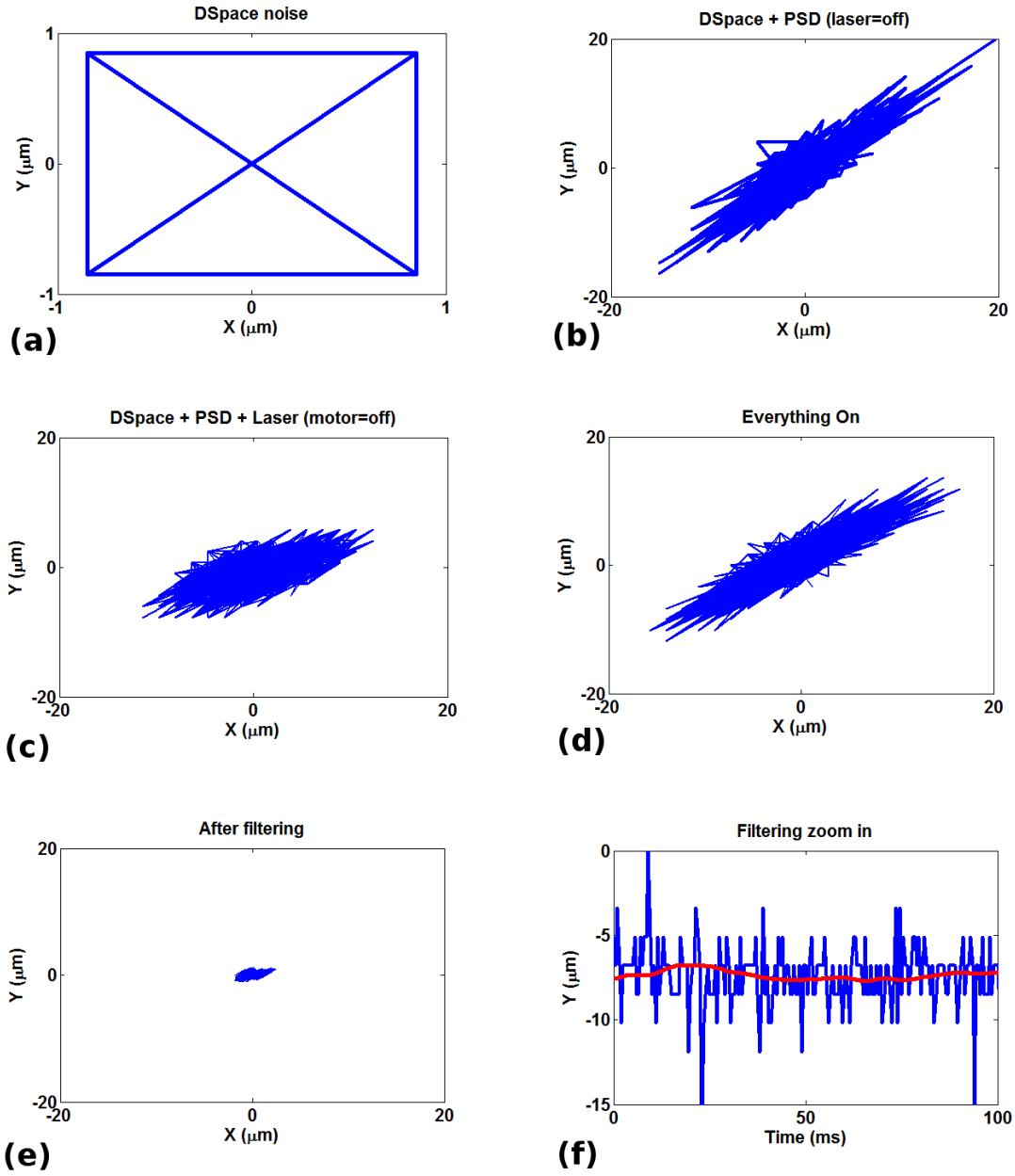

Figure 2.3: (a) The noise that dSPACE produces results in less than $1\mu m$ movement in each direction; (b) The noise of the system when there is not a laser beam on the PSD; (c) The noise of the whole system except the noise of the micro-manipulator motor; (d) The noise that the whole system produces when everything is on can be seen as an almost $15\mu m$ vibration in each direction; (e) The filtering has reduces the noise movement from $15\mu m$ to $1-2\mu m$ vibration in each direction; (f) A comparison of actual signal (blue) with the filtered signal (red graph in the middle) in an experiment.

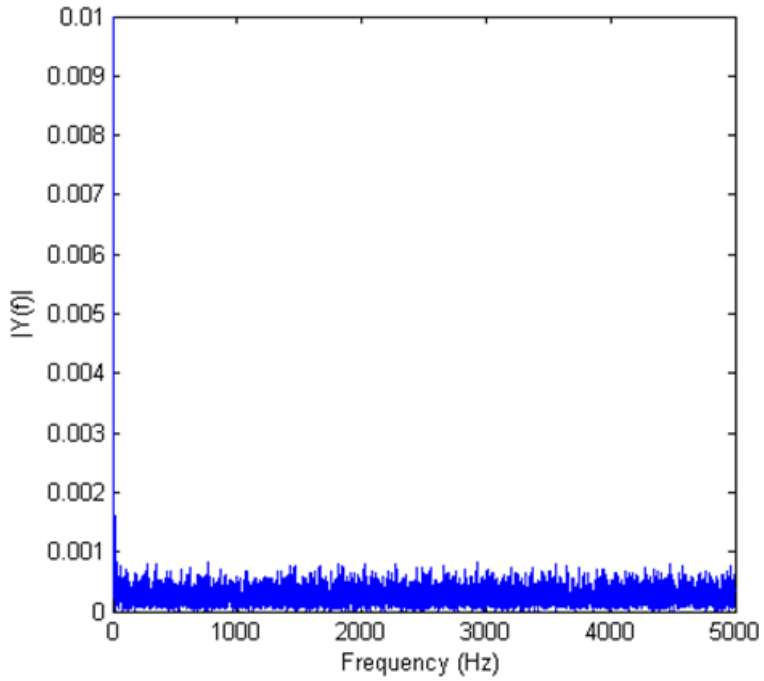

Figure 2.4: FFT of the noise of the whole system does not show any particular frequency for the noise to filtering it out.

By averaging a set of replicate measurements, the signal-to-noise ratio, S/N, will be increased [5]. To prove this, suppose the noisy signal v(k) is sampled every T seconds:

$$v(kT) = v_s(kT) + V_{noise}(kT) \tag{2.2}$$

If N partitions are composed, the averaged signal becomes:

$$\begin{gathered} y(kT) = \sum_{i=1}^{N} v_s^i(kT) + \sum_{i=1}^{N} v_{noise}^i(kT) \\ \forall k = 1, 2, ..., M \end{gathered} \tag{2.3}$$

If the partitions are perfectly aligned and the signal is truly periodic, the desired signal adds up:

$$\sum_{i=1}^{N} v_s^i(kT) = N v_s(kT) \tag{2.4}$$

However, for Gaussian noise with zero mean and a standard deviation σ_n (which also equals its rms value), we obtain

$$\sum_{i=1}^{N} v_{noise}^i(kT) = \sqrt{N\sigma_n^2} = \sqrt{N}\sigma_n \tag{2.5}$$

Taking the ratio of (2.4) and (2.4), we can find the signal-to-noise ratio (SNR) after averaging N partitions:

$$SNR_N = \frac{N v_s(kT)}{\sqrt{N}\sigma_n} = \sqrt{N} \times SNR_1 \tag{2.6}$$

Thus, we get an $\sqrt{N}$ improvement in the SNR.

As the previous figures have shown, the mean of the noise is zero and we know that signal and noise are uncorrelated so signal averaging is the perfect solution in this case. The only disadvantage of this method is that it produces some amount of delay based on the period we use for averaging. The Simulink® modeling of this filter is shown in Fig. 2.5:

Where gain block gives us $1/T$ where T is the time delay of transport delay block in seconds. The result shows significant improvement in noise reduction. The

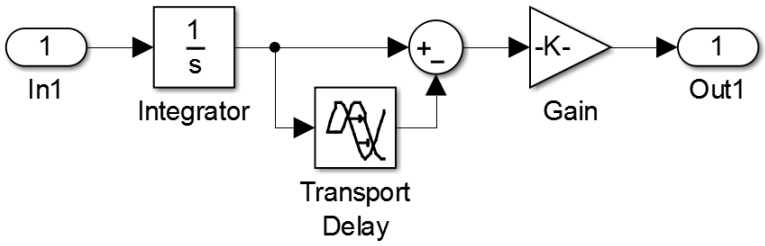

Figure 2.5: Filter model in the Simulink.

signal before filtering shows a vibration of about $15\mu m$ in each direction, but after the filtering, the movement is limited to $1-2\mu m$ in each direction. This has been achieved without losing actual data. The filtered signal follows the actual signal perfectly and the maximum delay is less than 50 milliseconds.

2.4.2 X-Y Mismatch and Rotation Correction

One of the problems with calibrating and actually using the data we get from the PSD is that the X and Y axes are not made perfectly perpendicular with each other in the PSD and also the PSD is not parallel with the motor that moves the laser. The first problem results in data that are not matched in just one direction and the second problem results in data that seems to be rotated a little bit. Notice that if the micro-manipulator axes were not perpendicular too, it would result in the same problem as the first one. To match the two Cartesian coordinates that are on the PSD chip surface and on the position sensing software interface, a rotation matrix $\left(\begin{smallmatrix} cos\theta & -sin\theta \\ sin\theta & cos\theta \end{smallmatrix}\right)$ has been used to correct the mismatch between the two coordinates, where $\theta = 2.29$ is the calibrated mismatch angle between the coordinates. Similarly, to solve the problem of the X and Y axes not being perfectly perpendicular on the surface of the PSD, a skew matrix $\left(\begin{smallmatrix} 1 & tan\varphi \\ 0 & 1 \end{smallmatrix}\right)$ was used, where $\varphi = -2.864$ was calculated. These corrections can be seen in Fig. 2.6.

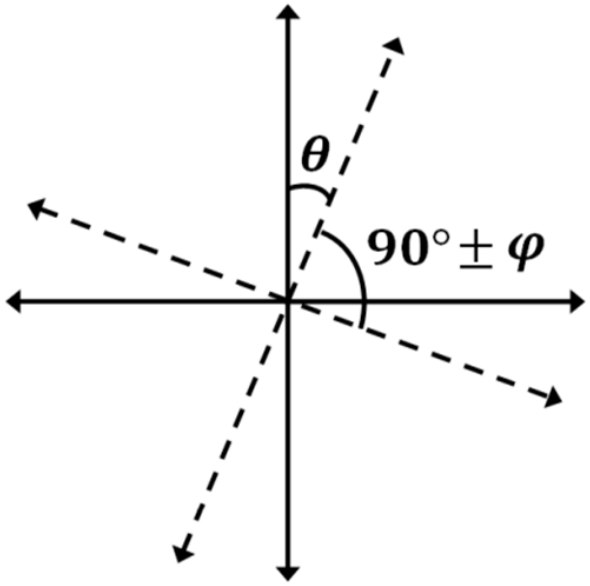

Figure 2.6: The effect of rotation and skew matrices.

2.4.3 Distortion Rectifying

The X and Y axes on the PSD have radial distortion. This means there is a deviation from the rectilinear projection. The type of radial distortion that the PSD has is called pincushion distortion. In pincushion distortion, the visible effect is that lines that do not go through the center of the image are bowed inwards, towards the center of the image. For correcting this distortion, Brown's distortion model [6] can be used. In this work, a version of the Brown's distortion presented by Villiers [7] with a slight modification was used:

$$\begin{aligned} x_u &= (x_d - x_c)(1 + K_1 r^2 + K_2 r^4 + ...) \\ y_u &= (y_d - y_c)(1 + K_1 r^2 + K_2 r^4 + ...) \\ r &= \sqrt{(x_d - x_c)^2 + (y_d - y_c)^2} \end{aligned} \tag{2.7}$$

Where (x_u, y_u) is the undistorted point, (x_d, y_d) is the distorted point, (x_c, y_c) is the center of distortion and $K_n = n^{th}$ radial distortion coefficient. For this distortion,

$K_1 = -0.62$ and $K_2 = 0.28$ were measured.

2.4.4 Mapping Validation

To evaluate the mapping performance after the coordinate rotation, correcting X-Y mismatches and rectifying the distortion, the laser diode mounted on the 3-D precision moving stage was used to generate various laser traces onto the PSD. In Fig. 2.7, a meander pattern was used to scan the whole surface of the PSD using the micro-manipulator as the reference. It became clear that the distortion is very noticeable. Using the above-mentioned corrections on the previous X_s and Y_s, the rectifying can be applied. The result as the rectified graph that is presented in Fig. 2.8 shows a very good mapping with the reference. It was measured that the mapping errors in X and X are less than $20\mu m$ which means less than 2%. The results clearly verify the good mapping performance by using the developed methods.

The meander pattern presents an acceptable distortion rectifying but it is actually a graph that just one of the parameters of X or Y changes at a time. To scan the biggest area as possible of the PSD surface an Archimedean spiral was used. This spiral can be shown using this formula:

$$x^2 + y^2 = a^2(tan^{-1}\frac{y}{x})^2 \tag{2.8}$$

The result presented in Fig. 2.9 verifies the previous finding and both mapping errors in X and Y within the range of $1mm$ are less than 2%.

2.5 The Scanning PSD Microscopy

After achieving a PSD system with high reliability and accuracy, a new scanning PSD microscopy can be extenThe microscopy is based on the vanishing effect and multi-channel photocurrent feedback mechanism of the accuracy improved PSD. In this section, we will detail the findings on this new microscopy.

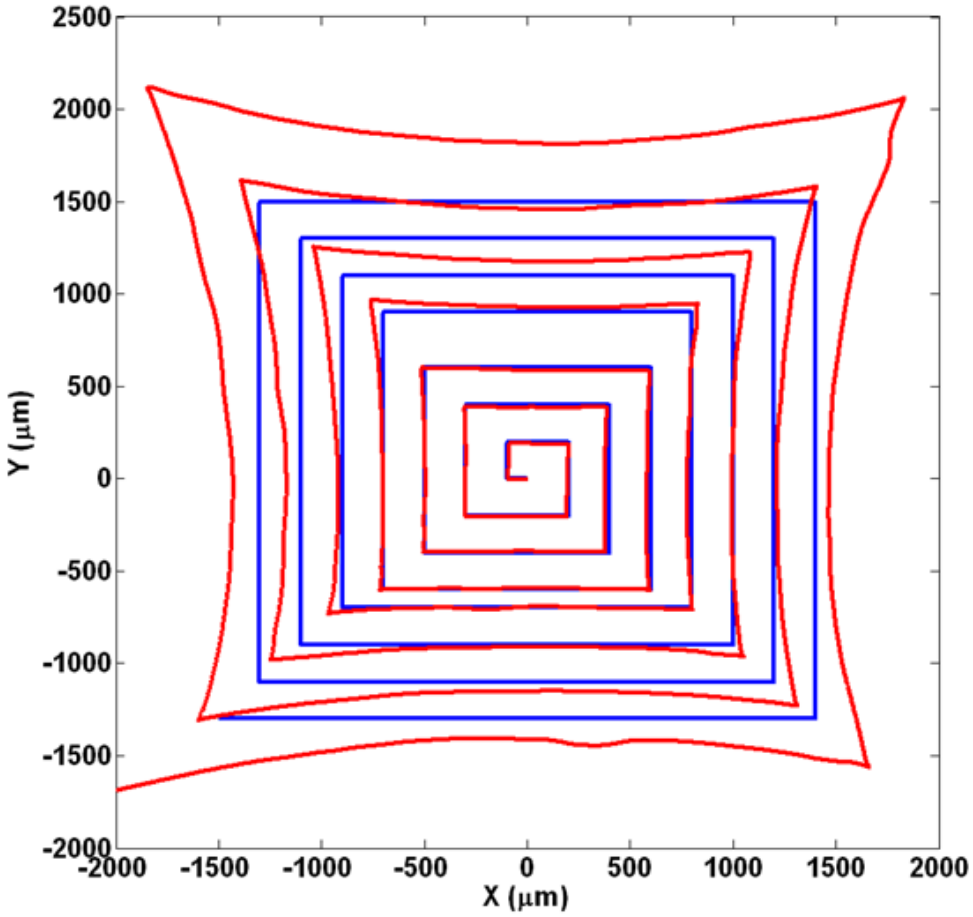

Figure 2.7: A meander pattern was used to determine the distortion (the red bigger graph). The blue graph is the reference.

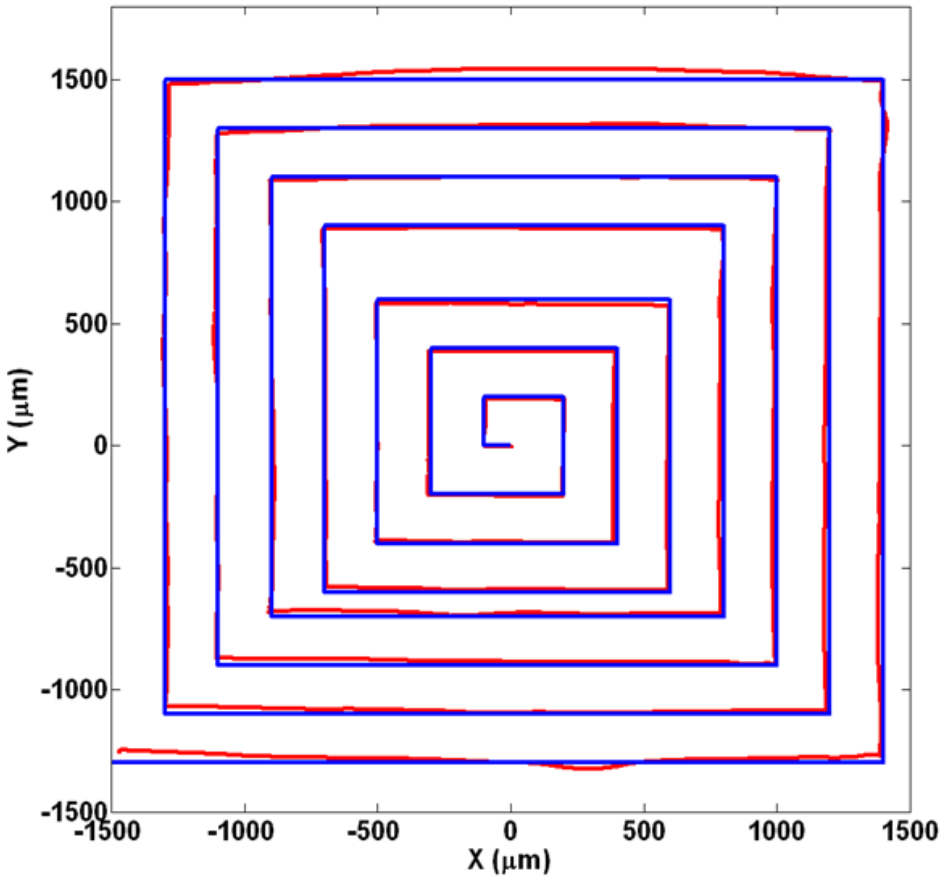

Figure 2.8: signal after rectifying (red) versus the reference (blue).

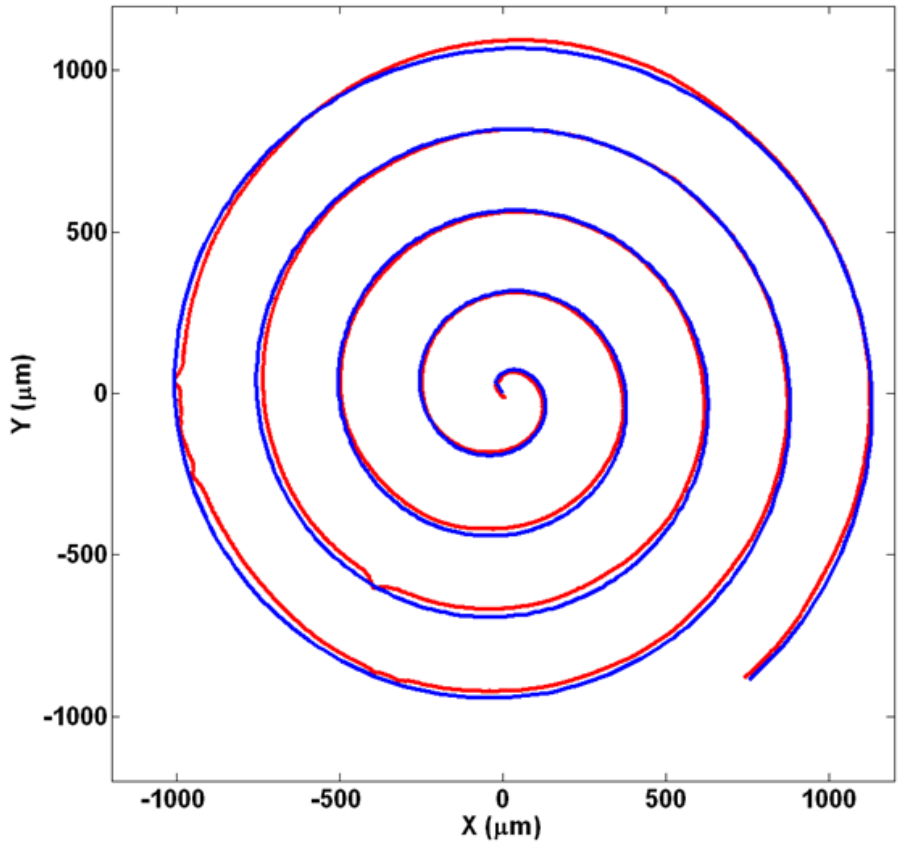

Figure 2.9: Archimedean spiral was used to verify the results. Blue is the reference and the red is the rectified signal.

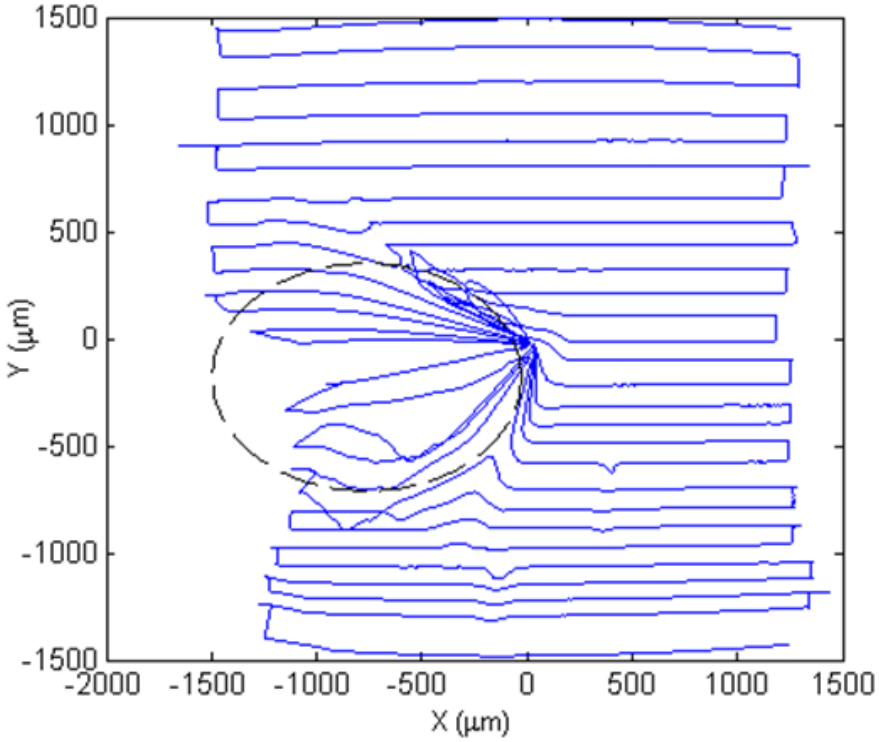

Figure 2.10: The broken lines represent a small object that was placed on the PSD. The effect can be seen as blue lines.

2.5.1 Photo-current Output and Vanishing Effect

After different tests, it became clear that the effect of blocking the laser beam can be determined by processing each of the 4 channels of the PSD individually. It was found that when there was a laser beam on the PSD, regardless of the position of the beam, each channel gives an output voltage of less than zero (because of the inverters in the PSD board) but when the light was blocked, they all quickly jump to zero. This effect can be easily seen in Fig. 2.10.

Based on this finding and the measurement accuracy improvement methods, a

scanning PSD microscopy is proposed and preliminarily implemented. The mechanism of the microscopy is based on processing 4 photocurrents from 4 input channels A, B, C, and D of the PSD and the developed accurate PSD mapping methodologies. Different methods were used to determine the exact point that the blocking of the laser occurs.

2.5.2 Three Methods for Finding Blocking Positions

Method 1

The first and the most accurate method is to monitor the smallest changes in two channels that are on opposite sides of the PSD. Using the property that was discussed in section 2.3, it is known that these channels have inverse correlation meaning that when one of them increases, the other one decreases. On the other hand, from the previous section, it is known that when an object blocks the laser beam, each channel immediately jumps to zero. This means they no longer have an inverse correlation. These facts are presented in Fig. 2.11 and are used in the first method.

The program works as it starts monitoring each channel from the beginning and as it determines that the channels are no longer in an inverse correlation, it marks that point as the starting point of the block and with a similar approach, finds the stopping point. By calculating these two points, it can correct the data in between and gives us the size of the object. This determination can be found out easily with this formula:

$$((A(i) - A(i-1)) \times ((B(i) - B(i-1)) < 0 \tag{2.9}$$

Notice it has been supposed that each current is uniform and changes smoothly but in practice, it is not the case. As a result of this, the smallest noise can ruin this method and gives a false positive. To overcome this problem, the program first finds a peak in one of the channels and then goes back to find the starting point. Unfortunately, this approach makes the first method unusable in online plotting as it needs to go back and forth in time. That is the reason for implementing the second

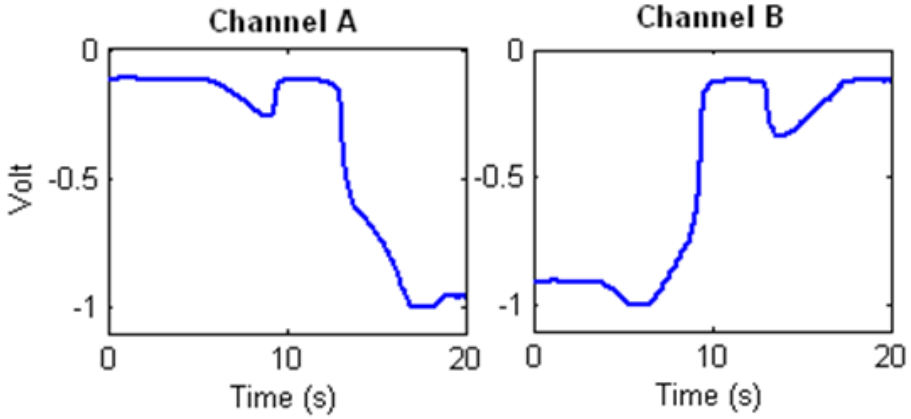

Figure 2.11: The inverse correlation and jumping to zero can be seen here. The laser has started passing an object from second 10.

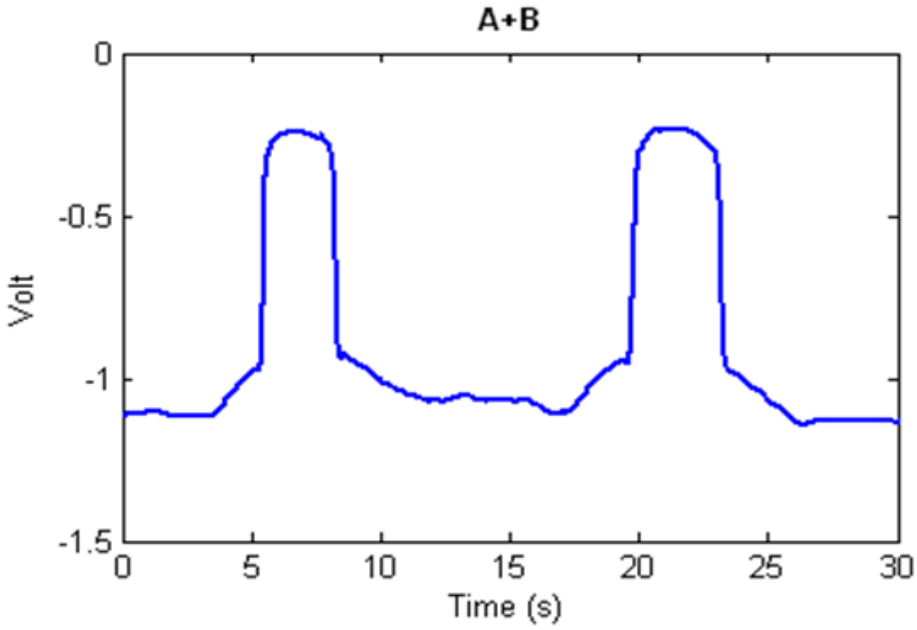

Figure 2.12: Two passes leave a clear effect on A+B.

method.

Method 2

The second method determines the starting and stopping points by monitoring $A + B$. The reason is, as it can be seen in Fig. 2.11, the inverse correlation between two channels can eliminate each other when added together in normal situations but when a block occurs, the addition of these channels can add up resulting in a bigger peak. This method is a bit less accurate as an exact specific point cannot be determined for every case but the advantage is that it can be used to correct the data online and generate the plots simultaneously. In this method, each time that $A + B$ becomes bigger than a specific set number (in this case, -0.9), a pass is marked and the starting and stopping points of the block can be extracted easily. Fig. 2.12 presents the effect of two passes on $A + B$.

The second method covers most of the situations unless the object is transparent. In such a case, the laser beam would not be blocked completely and the result would be just some disturbance. Monitoring $A + B$ does not help as it does not clearly become bigger than a set point so the third method was designed.

Method 3

The third method uses the fact that when an object, even a transparent one, blocks the laser beam, there would be a disturbance in both A and B. To monitor this disturbance, the derivative of $A + B$ was used to find the point that $A + B$ starts changing rapidly. These sudden changes in $A + B$ determine a disturbance and consequently a pass. Fig. 2.13 shows both channels A and B when the laser passes a transparent object. Fig. 2.14 shows that the derivative of $A+B$ has some considerably big peaks at the same time. This is because of the fact that it is showing the sudden changes in $A + B$ which is a result of the disturbance in each of the channels.

In the end, all three methods were used to find the starting and stopping points of each block. Based on these times and as the X and Y positions of the beam for any given time is known, the program can calculate the distance that the laser beam was blocked meaning the dimensions of the object.

2.5.3 Measuring from Scanning

At this point, we have all the requirements to measure the dimensions of an object. An experiment was designed to verify this ability. In this experiment, an SMD capacitor ($1.57mm \times 3.05mm \times 1.57mm$) was placed on the PSD surface. The laser performs a basic scanning and passes the object three times and the program uses the above-mentioned methods to find each blocking of the laser beam. The results and measurements for both channels A and B can be seen in Fig. 2.15.

Using the time of the starting point and stopping points of each pass, the program also shows the passes on an X-Y plot alongside the measurements of the object dimensions. This can be seen in Fig. 2.16. Note that in this figure, broken lines were

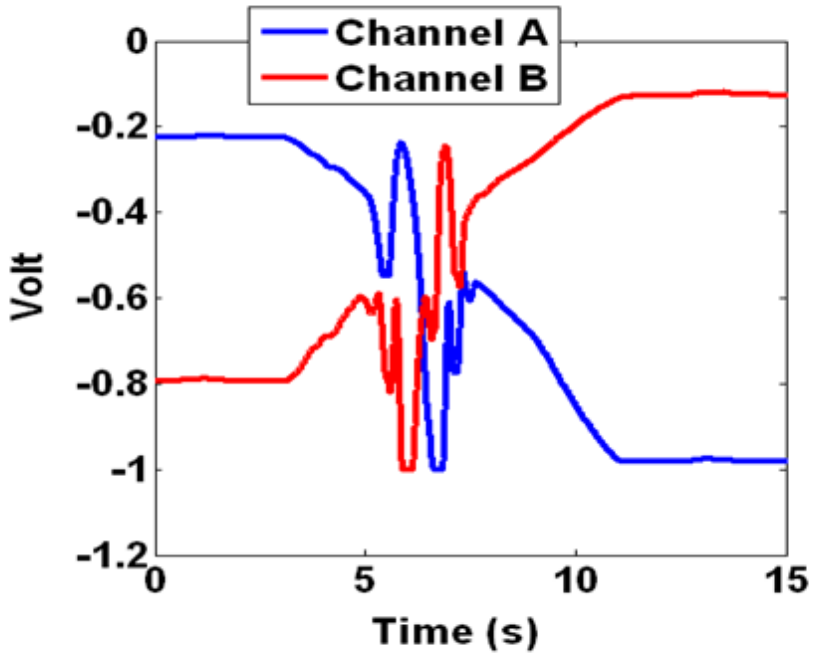

Figure 2.13: A pass of the laser over a transparent glass shows only a disturbance.

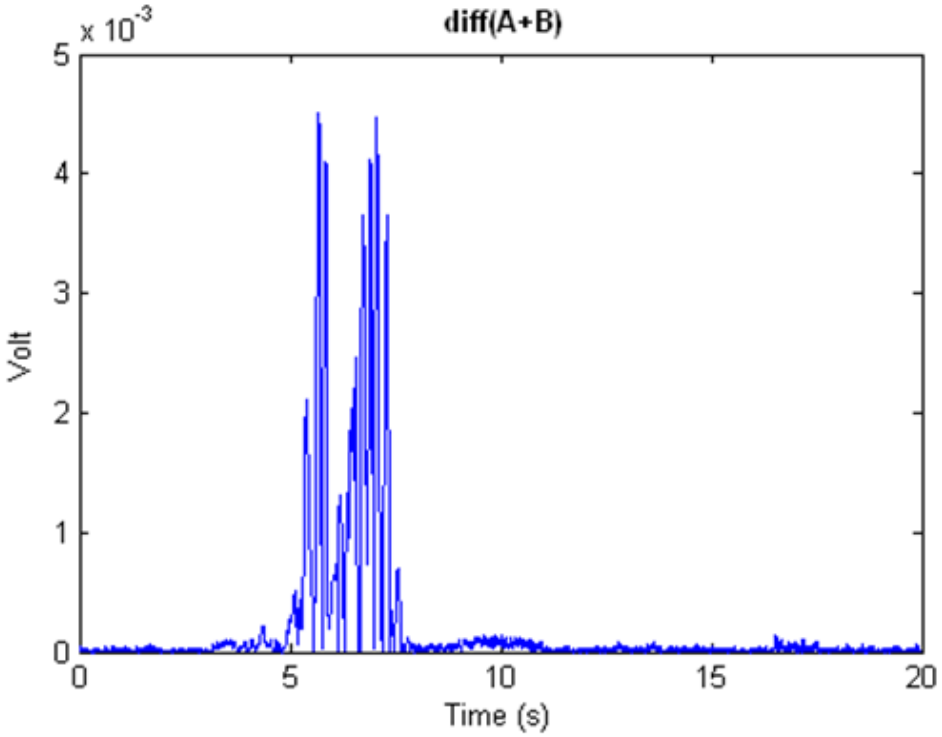

Figure 2.14: The derivative of v shows a disturbance from second 5 meaning a pass that lasts for about 2 seconds.

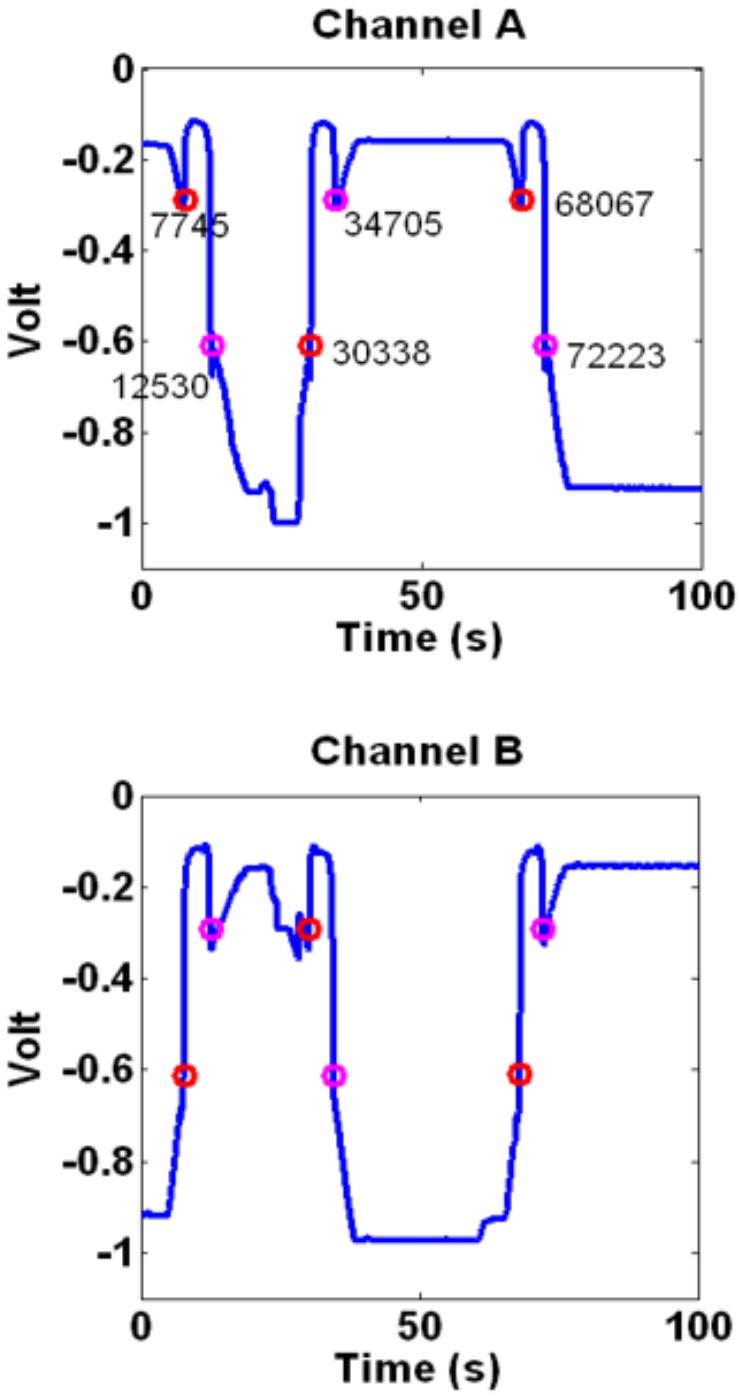

Figure 2.15: The program finds the starting and stopping points for each passes of the laser beam over the object. Here there are three passes over the object.

added later to represent the actual position of the object on the surface of the PSD.

After extensive experiments with different objects, it was determined that the measurements are promisingly accurate. Repeating the result gives a standard deviation of less than $6\mu m$ and the error in the full range is less than 4%. It should be noted that the diameter of the laser beam we used is about $1mm$ itself. So by using a laser that is capable of producing a smaller beam and focusing it properly, the measurements could improve significantly.

As it was discussed before in section 2.5, there is a method for performing the same measurements for transparent objects. To verify that, another experiment was designed. In this experiment, a glass micropipette with an outer diameter of exactly $1mm$ was placed on the surface of the PSD and the laser beam scans the surface once from side to side. By monitoring the derivative of $A + B$ the pass can be identified and can be seen in Fig. 2.17.

Different experiments measured the size of the transparent glass micropipette was repeatable with an acceptable error and as prior experiments, with a standard deviation of less than $6\mu m$. This shows that even transparent objects can be measured with this method. It is very important to note that these experiments are just preliminary proof-of-concept examples to test the abilities of the system and introducing a new method of microscopy. There are some problems with these experiments that makes the final conclusion on the accuracy a little dubious. For example, these experiments were done without a good certainty that the objects are perfectly parallel to the channels. A slightly rotated object can cause the system to find different values for its dimensions as the laser beam is now not perpendicular to the sides of the object and it is more like a diagonal path that enters one side and exits another one with an angle. Another problem is that in these experiments, we used SMD resistors as an object and the dimension of different resistors might not exactly follow the suggested dimensions of the datasheet. Others factors might influence the result too. But the fact that the results are repeatable with very small error and standard deviation, proves that the system is promisingly working.

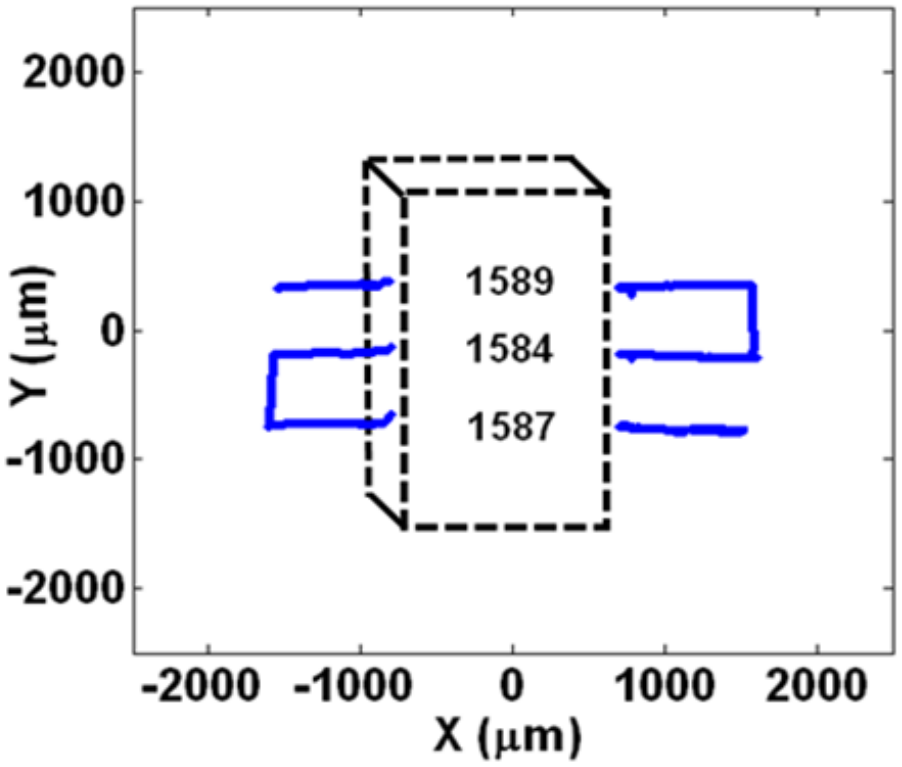

Figure 2.16: The program outputs an X-Y plot of the path that laser beam has travelled. Broken lines were added later to represent the object that was on the PSD surface.

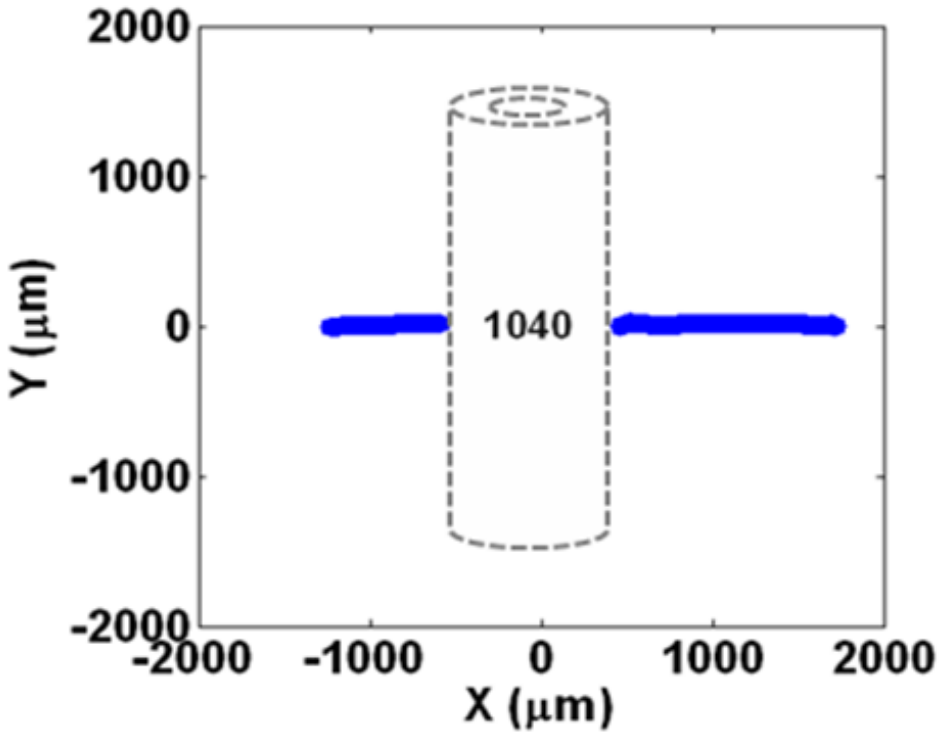

Figure 2.17: X-Y plot of the laser beam when passes over a transparent glass micropipette. Broken lines were added later to represent the object that was on the PSD surface.

2.6 Conclusion

This work was started by studying a Position Sensitive Device (PSD) and its characteristics. We then examined and analyzed noises that the system is facing and used the signal averaging to greatly minimizing these noises. In addition, the X-Y mismatch and rotations were addressed, the PSD distortion was examined and the Brown's model was used to rectify the pincushion distortion. Different tests were run to verify and test the mapping of the data after all the corrections. Later, the effects of blocking the laser beam were examined. Three different methods were designed and implemented to determine a laser block. In the end, a new method called Scanning PSD Microscopy was proposed to measure objects' dimensions on the PSD surface. Numerous tests were run to examine the feasibility and finding the accuracy of the measurements. It proves that the system is able to measure various objects, even a transparent object, with excellent accuracy and precision. The standard deviation of the measurements are less than $6\mu m$ and can be significantly improved by using better equipment.

Chapter 3

Adaptive Local Scanning: A Comprehensive and Intelligent Method for Fast Scanning of Indiscrete Objects

3.1 Abstract

A pixel-by-pixel scanning that is usually performed by a single point-like sensor or probe is being widely used in the applications such as scanning probe microscopy techniques. Typically their scanning time is several seconds to minutes long due to a raster scanning that needs to be conducted for capturing every single point on the surface of the sample area. To improve the scanning efficiency, recent research has been focused on investigating effective scanning patterns and methods. This work presents an adaptive local scanning method for efficiently sampling indiscrete objects like string-like one-piece connected objects under the microscopy. An initial scanning pattern is firstly investigated. Once the initial scanning reaches the object, an adaptive sinusoidal scanning method that can on-line adjust its scanning frequency and amplitude by predicting both the curvatures and the shape of the object is then developed and applied. The method also addresses scanning intersections and bifurcations associated with objects. Based on extensive implementation, it was validated that our method has high performance as it has high scanning efficiency and the scanned results match objects with high precision and high accuracy.

Keywords - local scanning, adaptive method, indiscrete objects, scanning patterns, microscopy

3.2 Introduction

Scanning using a probe has applications in various systems. One of the most famous applications is in Scanning Probe Microscopy (SPM) techniques [8]. In these systems, especially in Atomic Force Microscopy (AFM) scanning, a nano-scaled probe has to pass over the entire scanning area in a zigzag raster pattern to get the desired scanning image from the object. This approach, although being accurate, is considered time-consuming.

There have been many instances where research has been done in this area by investigators to minimizing the scanning time [9] [10] [11] [12]. In general, spending a long time in the scanning is inevitable in some cases but there are numerous situations that this time can be shortened greatly. In most cases, the area taken up by the object is significantly small in comparison to the whole scanning area. This would result in spending time on scanning uninterested regions. Local scanning methods arise to be one of the effective solutions but they generally depend on the form and shape of the target/object. Recently several interesting and important research has been reported by Chang and Andersson in [13] [14] [15] that the local scanning was successfully conducted on string-like objects such as nanowires, actin, and DNA strands. The assumption in these research works is that there is an open string-like object without intersections or bifurcations. The curve of the object is also assumed not to change very radically. Although these methods work very well in scanning an open-curved object, there are still some open problems in scanning objects that are not an open curve and have the form and shape with loops, intersections or bifurcations.

In this work, we address these open problems and develop and implement a comprehensive and adaptive local scanning algorithm that is capable of rapidly and accurately scanning the indiscrete, one-piece connected objects with various forms and shapes such as open or closed curves, loops, intersections or bifurcations, and so on.

More importantly, our algorithm and method do not require any prior information about the scanned objects. In addition, comparing to other existing local scanning methods that need a preparation or an initial scanning to know some prior information of objects before a regular local scanning, our method does not rely on any prior information about objects but points scanned on-line during the scanning. This will help to improve the scanning efficiency significantly. In other words, our developed method is intelligent and is more similar to a circumstance of a micro-mouse intelligently searching and finding the path. That is, the controlled micro- mouse solves a maze by keeping tracking where it is, discovering walls as it explores and mapping out the maze instead of having an already prepared map of the maze and just going through it.

In our algorithm and method, the first stage is to initially search the object in the scanning area. The initial search method is to help find one single point on the object. The initial search may be re-started in new areas if no point could be reached in the original area. Once the initial search path meets any point of the object, the second stage will start our adaptive local scanning from the scanned point. At the beginning, a sinusoidal scanning pattern with the set highest frequency and amplitude is applied toward an immediately calculated direction. As more new points of the object are being discovered along the direction, the scanning frequency and amplitude will be adaptively adjusted based on the object's curvature and thickness that can be predicted using previously scanned points. When abnormal points represent intersections and bifurcations on the object and a new local scanning will be started from those points. Once the local scanning is finished (no new point is found in the region of interest), the final stage is to use a parametric Fourier curve fitting method to optimize the scanned points. The fitting method helps to improve scanning accuracy by minimizing the scanning error to almost half of the original error. By implementing these stages combined with other developed algorithms such as "preventing double scanning", "determining the side of a curve" and "returning from a lost tracking", the results validate the high performance of the developed comprehensive and adaptive local

scanning method. The algorithms and method are being extended to a new scanning PSD microscopy system proposed by us [16]. Other applications include the fast AFM, SPM or laser scanning.

This paper is structured into the following sections: In Section 3.3, the effective initial search scanning is investigated and discussed. Section 3.4 introduces the develops adaptive local scanning algorithms and methods, including the sinusoidal scanning pattern, methods of resuming the scanning for the missed points, the scanning method for intersections and bifurcations, thick objects scanning, double scanning prevention, and the flowchart of the developed algorithms and methods. Section 3.5 presents one of the implementation results. In Section 3.6 we conclude the work.

3.3 Initial Search Scanning Pattern

The first stage of our scanning needs a very fast and effective scanning pattern to find the unknown object. It is required to search as many areas as possible in a very short time. As just one contact with the object is needed for this stage, the pattern should be widespread to increase chances of intersecting the object. There are many patterns used for different applications [17]. To find the best pattern, a simulation program was firstly developed and plenty of different patterns were tested. The program has various capabilities. Any pattern or object can be defined easily in the program. The program then simulates the pattern, measures how long it would take the micromanipulator to draw the pattern, and finally how many times the pattern has passed the object edges. This gives us a good scale to find out which pattern is faster and which pattern can scan more. A representation of this simulation can be seen in Fig. 3.1. Note that, besides a rectangle object, various objects have also been tested to prove the best pattern (i.e. Star-6).

An efficiency factor is defined as the number of passes over the whole time that a pattern takes. Also numerous patterns and different objects were examined. Finally, based on the efficiency factor, it was determined that Star-6 (a pentagram with one extra line) is the most efficient pattern. Table 3.1 shows the efficiency factor for

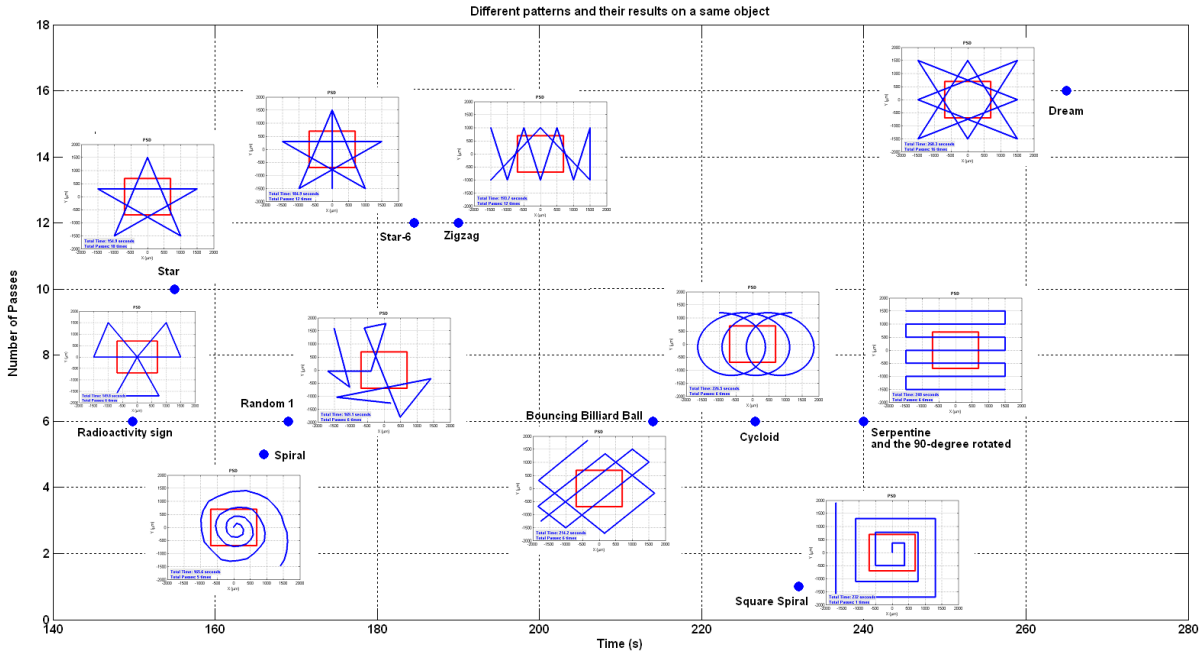

Figure 3.1: The most famous scanning patterns where tested by a simple rectangle object to find differences in scanning time and times of intersection.

different patterns in Fig. 3.1. To get the best pentagram, a pentagon inscribed a circle with radius R (that is half of a side of the scanning area) is needed.

Each side of the pentagon that inscribed a circle with radius R is defined with the equation 3.1:

$$2 \times R \times sin(\frac{\pi}{N}) \tag{3.1}$$

Where $N = 5$ is the number of sides.

A simple pentagram pattern would find any object that has the same shape as the scanning area and is bigger than 12% of the whole area. But to be sure that smaller objects would not be missed, a second rotated Star-6 pattern will be performed after the first one. This would continue with a third scaled down one to be sure that even the smallest object would not be missed. By using all these sequences, an object should be smaller than 4.2% of the scanning area to be missed. Notice that as soon as one of the patterns has an intersection with the object, the algorithm would not

Table 3.1: Comparison Between Different Patterns In Fig. 3.1.

Pattern	Time	Passes	Efficiency factor
Star-6	185	12	6.49
Star	155	10	6.46
Zigzag	194	12	6.2
Dream	268	16	5.96
Radioactivity	150	6	4.0
Random 2	219	8	3.56
Random 1	169	6	3.55
Spiral	166	5	3.02
Bouncing Billiard Ball	214	6	2.8
Rotated Serpentine	240	6	2.5
Serpentine	240	6	2.5
Square Spiral	232	1	0.43

continue the other ones to save time as no other scanned point is necessary.

3.4 Adaptive Local Scanning Methods

3.4.1 Defining a Sinusoidal Scanning Pattern

The outcome of the previous stage is to reach the first point of the object. Once the first point is met, a sinusoidal pattern scanning will be started from this point. To map a sinusoidal pattern, a line is needed and to get a line a second point of the object should be found. To achieve this, a circular search with the first point as the center would be performed to find the second point. This circle would eventually intersect the object, giving the second point of intersection. The circle is defined in the equation 3.2:

$$\begin{gathered} 0 \leq ang \leq 2\pi \\ CircleX(ang) = IntersectPoint + Radius \times cos(ang) \\ CircleY(ang) = IntersectPoint + Radius \times sin(ang) \end{gathered} \tag{3.2}$$

By having these two points and using extrapolation, the first tangent vector of the object can be found. This work has been implemented in MATLAB® but the ready-to-use interpolation functions of MATLAB can be sometimes bothersome. Instead, adding unit vector to one of the points to get the line was used and it is defined as follows:

$$\begin{gathered} \hat{u} = \frac{u}{|u|} \\ LineX(k) = k \times \hat{u}_x \\ LineY(k) = k \times \hat{u}_y \\ \forall k = 1, 2, ..., n \end{gathered} \tag{3.3}$$

Using this tangent vector, a sine wave is mapped to the line to get the scanning pattern. The sine wave is given as:

$$x(t) = \hat{x_d}(s(t)) + Asin(\omega s)q(s(t)) \tag{3.4}$$

Where the amplitude A and frequency ω are pre-defined values for the first scanning pattern. They may adaptively change to follow the predicted form and shape of the object. The details will be described in later sections. Each time that the pattern intersects the object, a new point has been found and by using this new point, a new tangent vector and scanning pattern would be defined. This would let the pattern to follow the object very smoothly as it turns. The algorithm also monitors the time that pattern takes between two consequent points. Based on this, the amplitude would increase or decrease to match the object and save more time by not using a too high amplitude when it is not needed.

The problem may arise that if the frequency does not change, it is likely that the pattern misses the object around a very sharp turn. This problem can be seen in Fig. 3.2. To solve this, the frequency needs to increase when the pattern is approaching a sharp turn. To determine a sharp turn beforehand, the algorithm monitors the changes in the angle of the tangent vector for each point and compare it to the same angle of the previous points. This would let the algorithm to predict a sharp turn based on previous information. For example the angles of the tangent vector for the few last points of Fig. 3.2 before the curve are: 348.4, 343.3, 344.5, 338.5, 326.8, 309.3 degrees so the differences between each two consequent points are: 5.1, 1.2, 6.0, 11.7, and 17.5. By just looking at these numbers it is obvious that a sudden change of angle is occurring, as a sequence of numbers around 4 are suddenly followed by 11.7 and 17.5. This immediate change in angle has a meaning of a sharp turn. By applying this method the object in Fig. 3.2 was scanned by the new pattern. This can be seen in Fig. 3.3.

3.4.2 Resuming the Scanning for the Missed Points

As it was mentioned previously when the initial scanning pattern finds an intersection with the object, it would start a circle scanning and the sinusoidal pattern would start from this newly founded point. This means that by finishing scanning of this part of the object, the other side of the object is still not scanned. At this point,

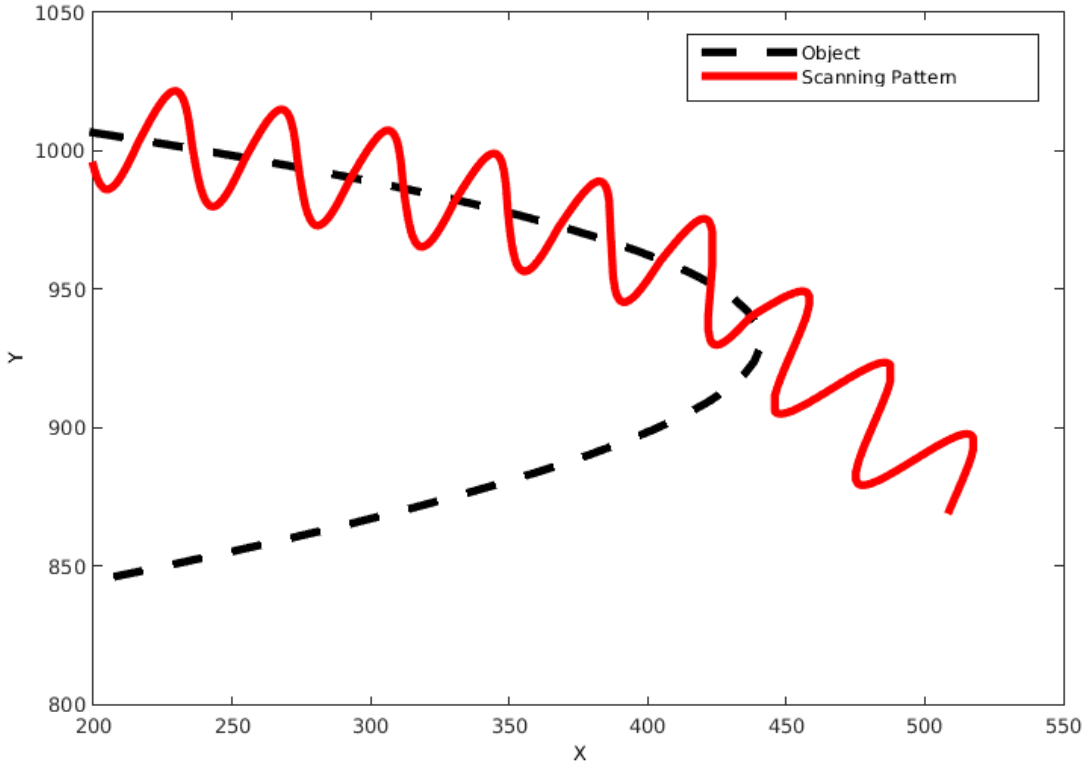

Figure 3.2: Shows that a constant frequency can miss the object even if the path is corrected with every new point.

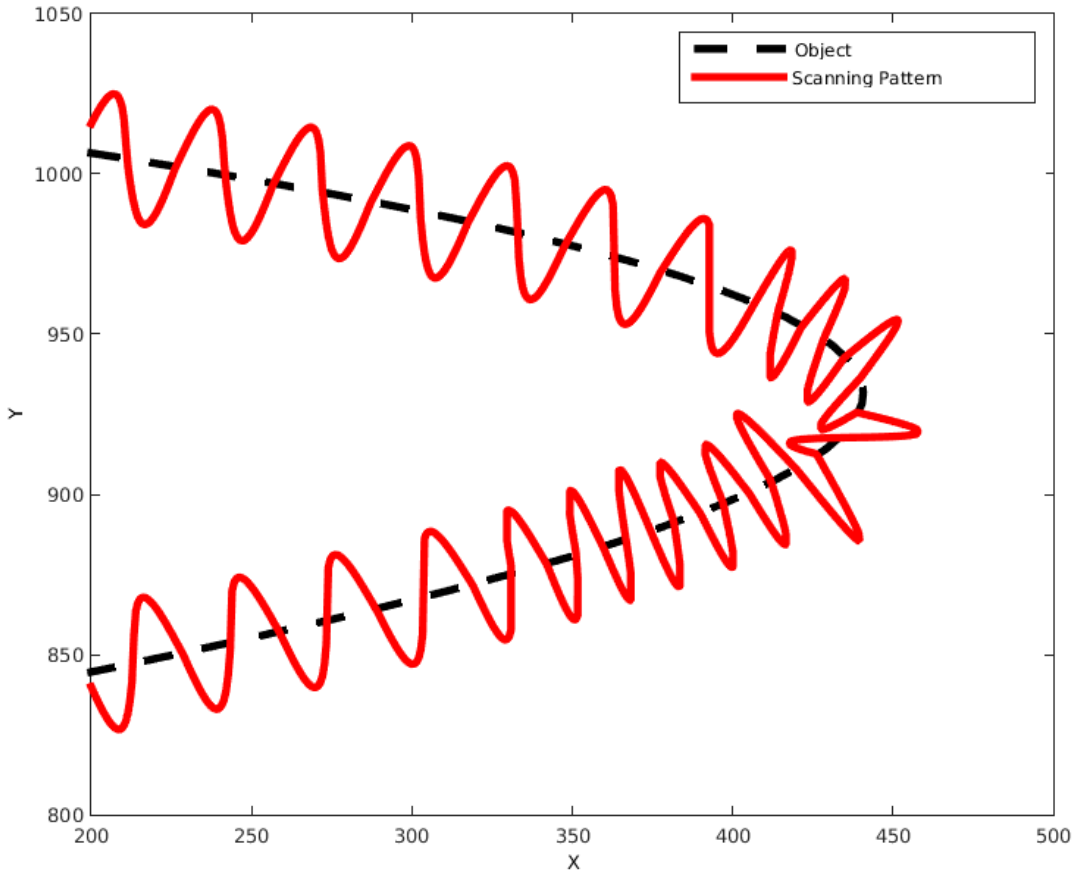

Figure 3.3: Illustrates that by monitoring changes in the angle of tangent vector and updating the frequency accordingly, this problem would be solved.

the algorithm would return to the starting point and resume the scanning toward the other side. Everything about the amplitude and frequency would apply to this scanning too. This way, both sides of the object have been scanned although the scanning was started from a random point-usually in the middle- of the object.

One problem is that even though the frequency is changing according to the curvature of the object, there are some rare situations that the turn is so sharp and sudden that even a scanning pattern with high frequency would miss the object. In these cases, a strategy for finding the object again is needed. To achieve this, when the pattern does not find any intersection points for a given amount of time, it would start a searching scan to get back to the object. An Archimedean spiral was selected as the searching scan. This gives the benefit of scanning an area around that point in one pattern only. The Archimedean spiral is defined by the following equation:

$$x^2 + y^2 = a^2(tan^{-1}\frac{y}{x})^2 \tag{3.5}$$

Or in parametric format defined as:

$$\begin{aligned} x(ang) &= b \times ang \times cos(ang) \\ y(ang) &= b \times ang \times sin(ang) \\ 0 &\leq ang \leq a \end{aligned} \tag{3.6}$$

When the searching pattern scans around a point, generally two points would be founded. One of them is the new point that the scanning would continue toward it and the other point is on that part of the object that was just scanned. By comparing these two points with all previous intersections, this can be distinguished. An example of a searching scan after a miss is shown in Fig. 3.4.

3.4.3 Intersections and Bifurcations

Not all objects are string-like form without any intersections and bifurcations. There are examples that the object has some intersections or bifurcations like Bifid Y-shaped cell that occurs most often in Gram-positive [18]. In these cases the scanning pattern

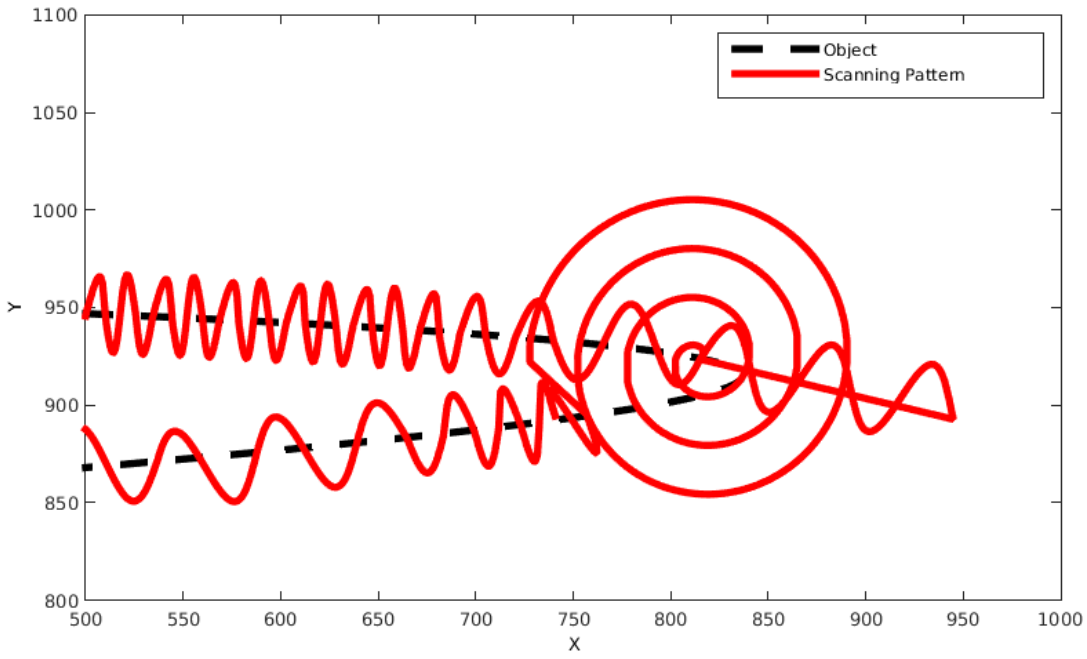

Figure 3.4: An Archimedean spiral searches for the object after the pattern misses the object due to a very sharp turn.

would continue toward one of the paths and the other path would remain without scanning.

Fortunately, there is a way to find these special points and return to them for another scan. Every time that the pattern reaches an intersection or bifurcation there would be a sudden change in the path that has no traces in previous points. By monitoring for these sudden changes that were not expected beforehand, the algorithm can find these special points. After finishing the scanning for both sides of the object, the algorithm would return to these points, performs a searching scan and continues the scanning from these points to find any path that has not been scanned before.

A common occurrence in these situations is that the searching scan would find a path that has been scanned before. To prevent this, any time that the pattern intersects the object, it compares that point with all previously scanned points to be sure that this is actually a new point and this path has not been scanned before. This "New point check" algorithm would stop the program from being in a loop even if the object is just a circle. An example of the bifurcation detection and searching scan is shown in Fig. 3.5.

3.4.4 Scanning Thick Objects

When the object is very thick, the side edges are very far from each other and the algorithm would face another problem. In these cases, the tangent vector of the two sequent points is not in line with the object and is almost perpendicular to the object. This would cause a lot of problems. To solve this, when the object is thick, one side of the object is selected randomly and any further correction to the sine wave would only apply if the pattern is on the same side. By using the following method it can be found out which side of the object is a dot located. To determine which side of the line from $A = (x_1, y_1)$ to $B = (x_2, y_2)$ a point $P = (x, y)$ falls on, d needs to be computed by the following equation:

$$d = (x - x_1)(y_2 - y_1) - (y - y_1)(x_2 - x_1) \tag{3.7}$$

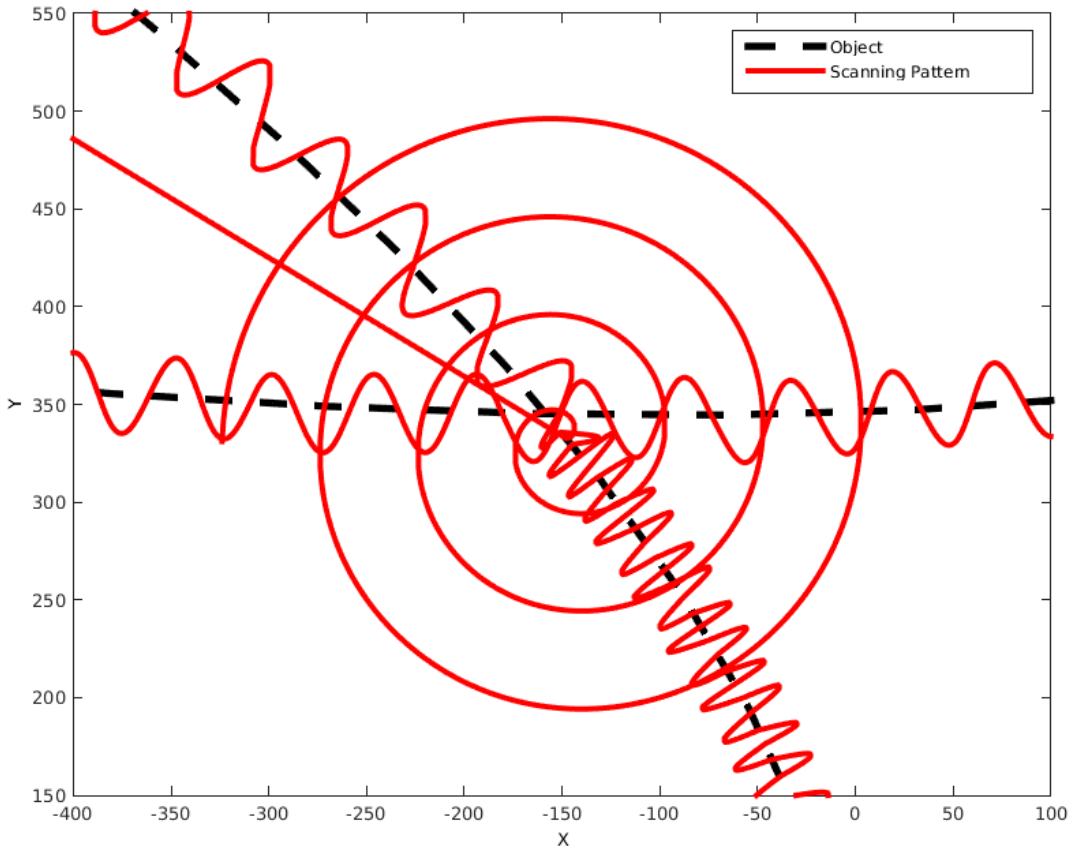

Figure 3.5: A searching scan is performed at an intersection and each path is scanned accordingly.

Where if $d < 0$ then the point lies on one side of the line, and if $d > 0$ then it lies on the other side. If $d = 0$ then the point lies exactly on the line. This is the simpler form of doing the actual method that if the point is given by the $2D$ vector $\overrightarrow{P}$ and the line end points by $\overrightarrow{A}$ and $\overrightarrow{B}$, then cross product is calculated as below:

$$\begin{aligned} \overrightarrow{AB} \times \overrightarrow{AP} &= x_{AB} \times y_{AP} - x_{AP} \times y_{AB} \\ x_{AB} &= x_B - x_A, \\ x_{AP} &= x_P - x_A, ... \end{aligned} \tag{3.8}$$

The sign of the above will determine what side of the line the dot is located. An example of a thick object and its scanning pattern is shown in Fig. 3.6.

3.4.5 Flowchart of the Developed Algorithms and Methods

The flowchart of the developed algorithms and methods can be seen in Fig. 3.7 which is presented in three different stages. The first stage starts with the initial searching scan and continues with finding the first point of the object. Then a circle search is performed to find the second point of the object. The first stage finishes here when it has two points of the object.

The second stage begins with defining a line that passes the two recently founded points in the stage one. This continues by the mapping of a sine wave to the line and adjusting its frequency and amplitude based on the distances of the scanned points. The scanning would be resumed until a new point of the object is found. At this point, the program checks for the tangent vector of the new line which is based on the founded point. If the program determines a sharp curve, it would correct the scanning pattern based on the curvature and if the curvature is too sharp, it would record that point for a spiral search in the third stage. The actual criteria for these decisions were found by experiment. By following the same rules, the scanning would continue until it cannot find any new points for a given amount of time which at that moment the program would perform a spiral search to be sure that this side of the object is finished and would continue to the third stage.

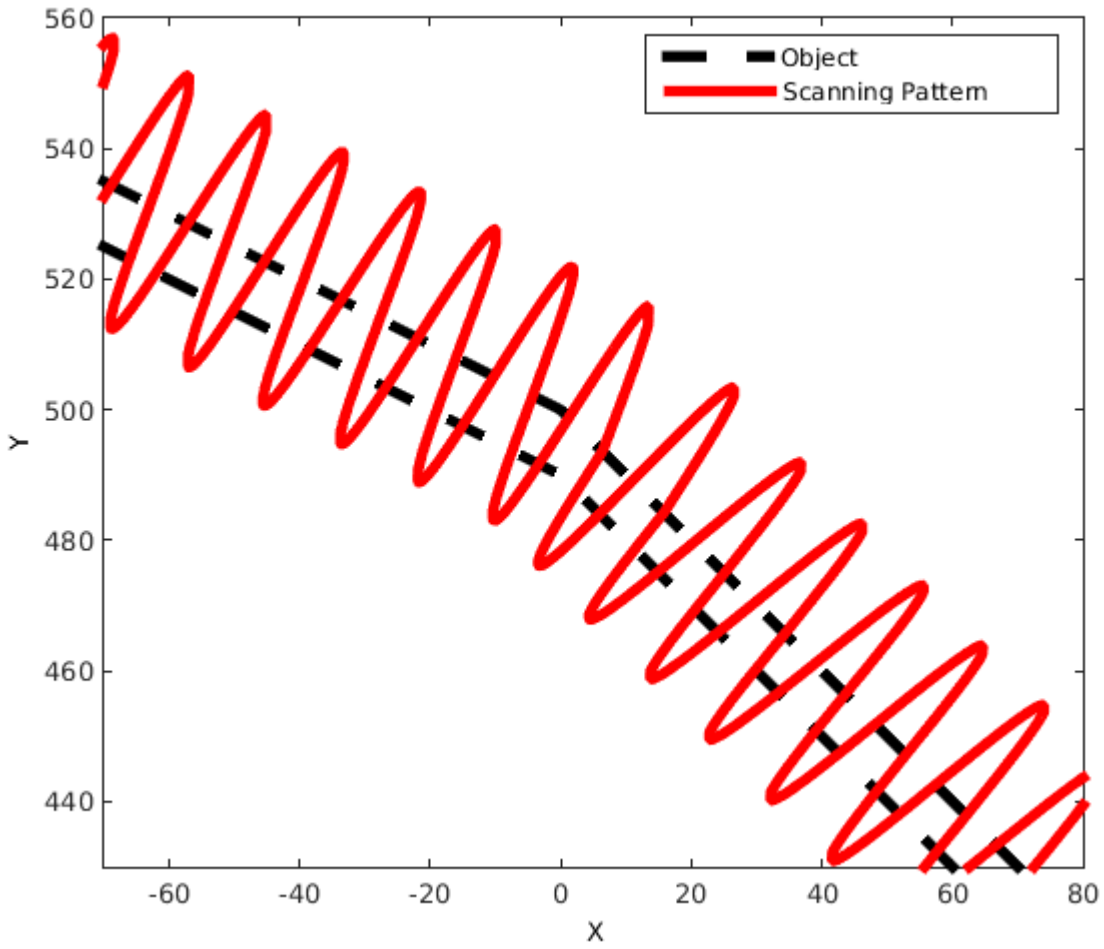

Figure 3.6: A thick object is scanned by choosing one edge as the correction side. In this figure, the upper edge has been selected automatically by the algorithm.

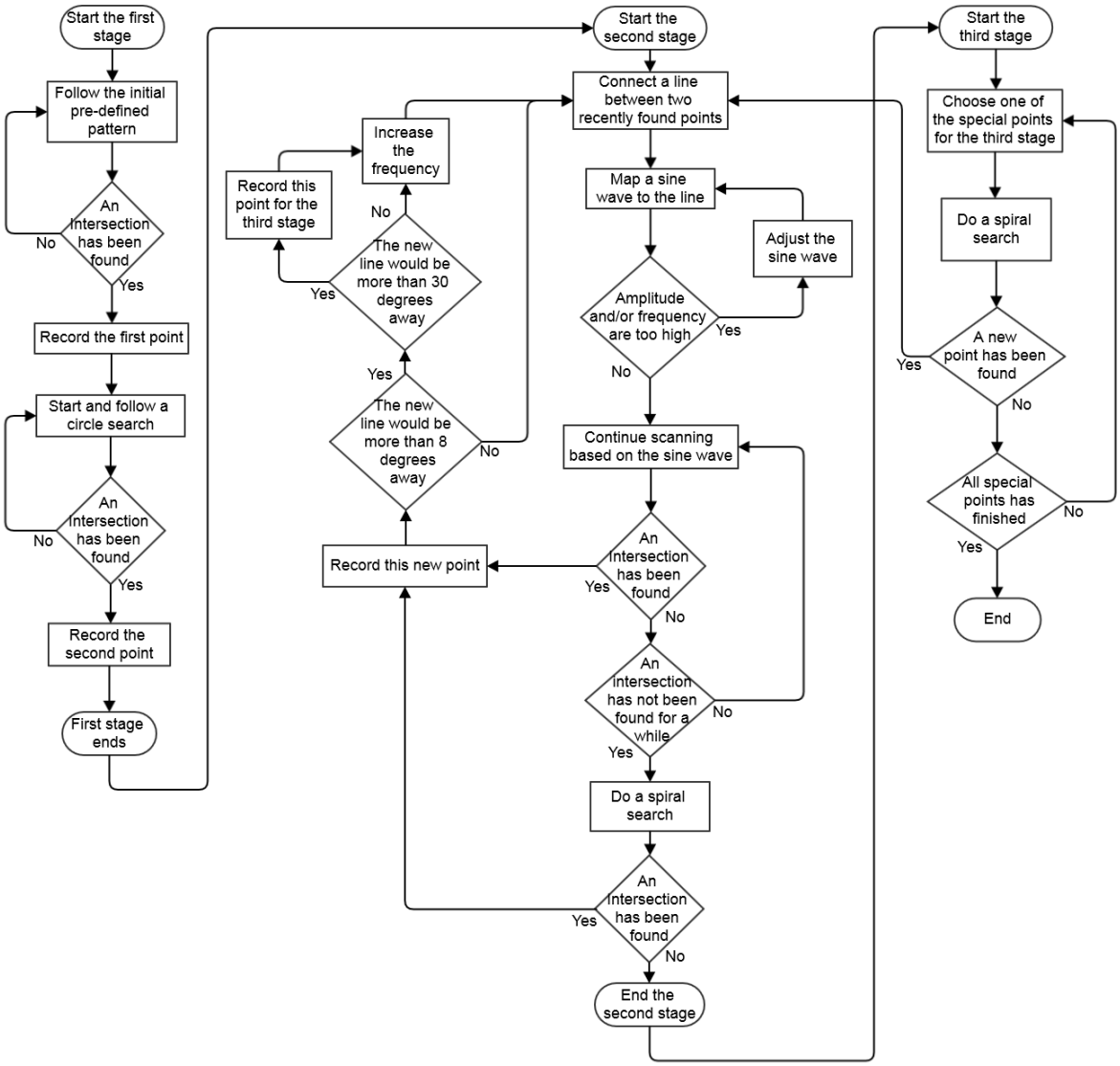

Figure 3.7: The flowchart of the algorithms and methods.

The third stage is when the algorithm needs to scan intersections and bifurcations again for any missed point. If by doing that, a new point is found, it would re-run the second stage based on this new point. This is to be sure that if a new path has been found at an intersection, the program would scan it thoroughly. It should be noted that this is a simplified version of the algorithm and putting all the different parts of the program in a single flowchart was not possible. When the algorithm scans all the special points and does not found any new points, the program finishes and presents the data.

3.4.6 Double Scanning Prevention

At this point, the algorithm can scan any object with inter- sections and bifurcations but there are instances where a path that starts from an intersection, goes back to the object at a different location. The program follows every path to be sure that it has scanned all the object. But following these paths might cause the program to scan a loop over and over.

A mechanism should be implemented to prevent the program of scanning a single location twice. To do this, a function checks every newly scanned point against all the previously scanned points. If a point could be found that is within a certain distance of the new point, this can be seen as a red flag of double scanning. To be sure that it is actually scanned before -and not just a point near another part of the object- a few of the recently scanned points is examined too. In case there was no doubt that this path was scanned before, the pattern would stop and goes back to another stage of the program.

3.5 Implementation And Verification

The points that the scanning pattern finds from the object are on the outer edges of the object. To get the actual object which is between these points, an interpolation would not be suitable for the exact same reason. Instead, a parametric Fourier curve fitting with 6 terms was used as shown in the following equation:

$$y = a_0 + \sum_{i=1}^{6} a_i cos(n\omega x) + b_i sin(n\omega x) \tag{3.9}$$

Where these coefficients a_0, a_i, and b_i in the equation are determined by the fitting function. Any number of terms more than this would result in over-fitting.

In addition, as the whole scanned points are obtained by a lot of sudden jumps to different positions -like scanning each side of the object or resuming the scanning for intersections and bifurcations- it is not possible and reliable for all the scanned points to be fitted at once. To solve this, the scanned points are divided into small parts by considering the jumps and sudden changes in directions. Each part is fitted separately and the final result is obtained by simply putting these pieces together. An example of the fitting and scanning pattern is given in Fig. 3.8 and Fig. 3.9.

To find out what is the difference between the actual object and the fitted curve and how the fitting is helping to get a better scan, a simulation was used. Although the algorithm does not have access to the position of the actual object, it can be used after scanning to compare the results with the actual values. This comparison is shown is Fig. 3.10.

Fig. 3.10 shows that the mean of the differences between scanned points and the actual object is 0.316 while the mean of the differences between fitted points and the actual object is 0.169. This shows that the accuracy has been doubled obviously. This fitting has a coefficient of determination of and only 9 points couldn't be fitted. Also, the object is defined in a square scanning area of 4000 points by 4000 points. The mean difference of 0.169 points between final results and the actual object shows the very high accuracy of the scanning algorithm and the fitting.

To present a comparison of the improvement in the scanning time, the pattern that scanned the object in Fig. 3.8 needed 27110 points for the probe to travel while -considering the 4000×4000 scanning area- a traditional raster scanning probe has to travel 16 million points to achieve the same results. This means this scanning time is 0.00169 of the traditional raster scanning time which means 590.2 times faster. Obviously, this great improvement is only achievable by using local scanning and

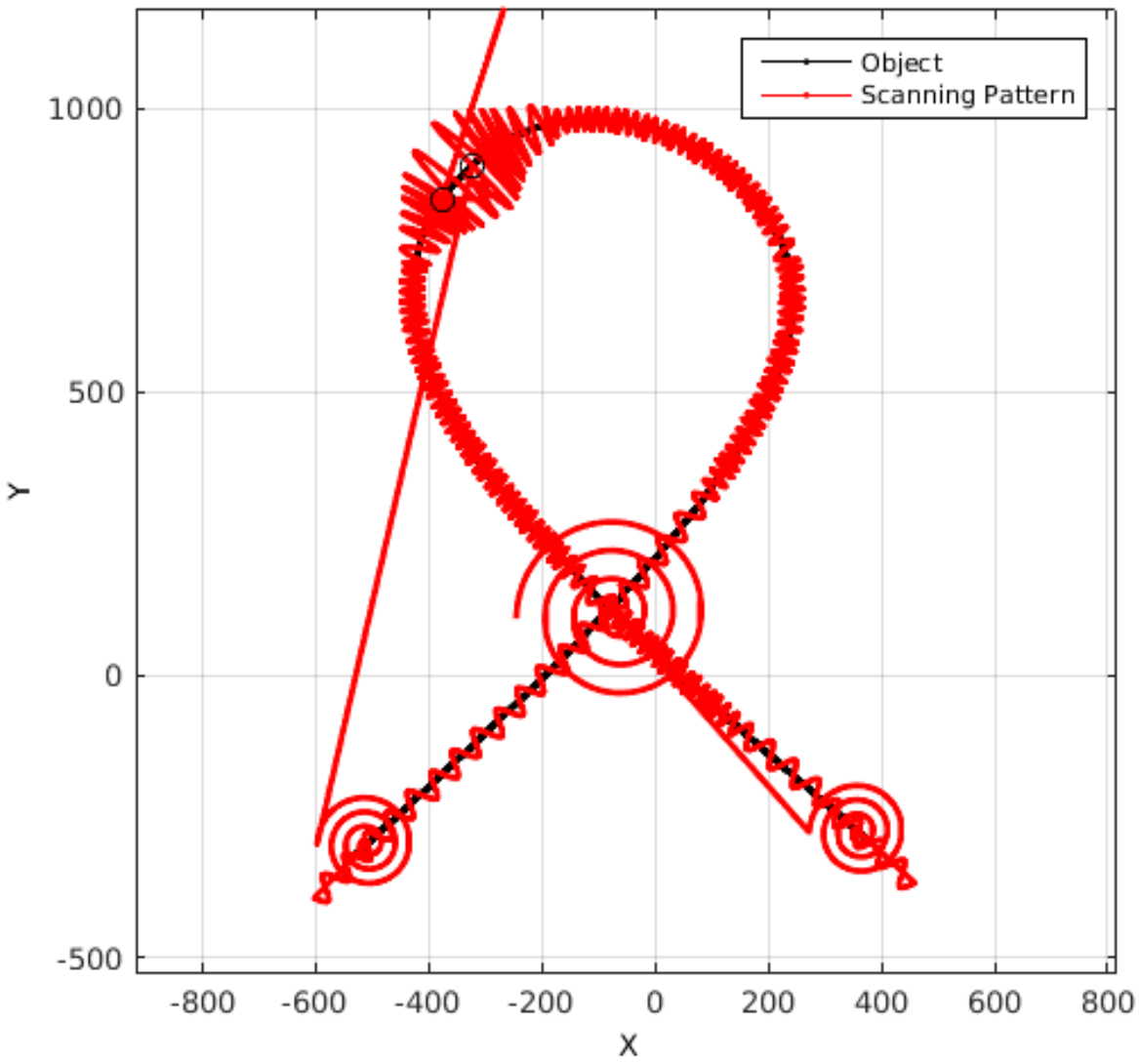

Figure 3.8: This figure shows an object and the scanning pattern.

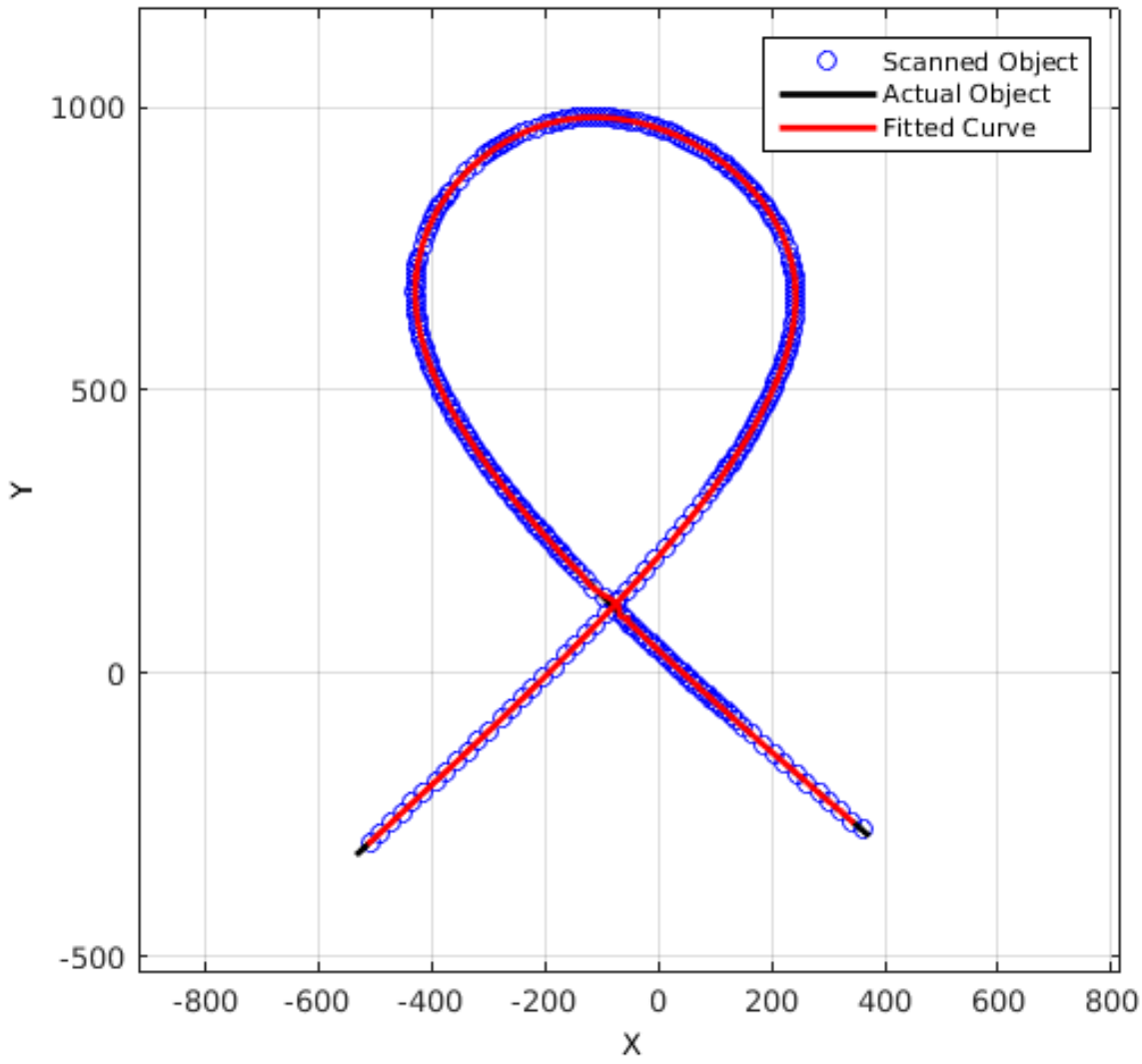

Figure 3.9: This figure displays the points that were obtained by the scanning and a fitted curve to those points. Note that as the fitted curve (in red) is very close to the actual object (in black), these two curves overlap in this figure.

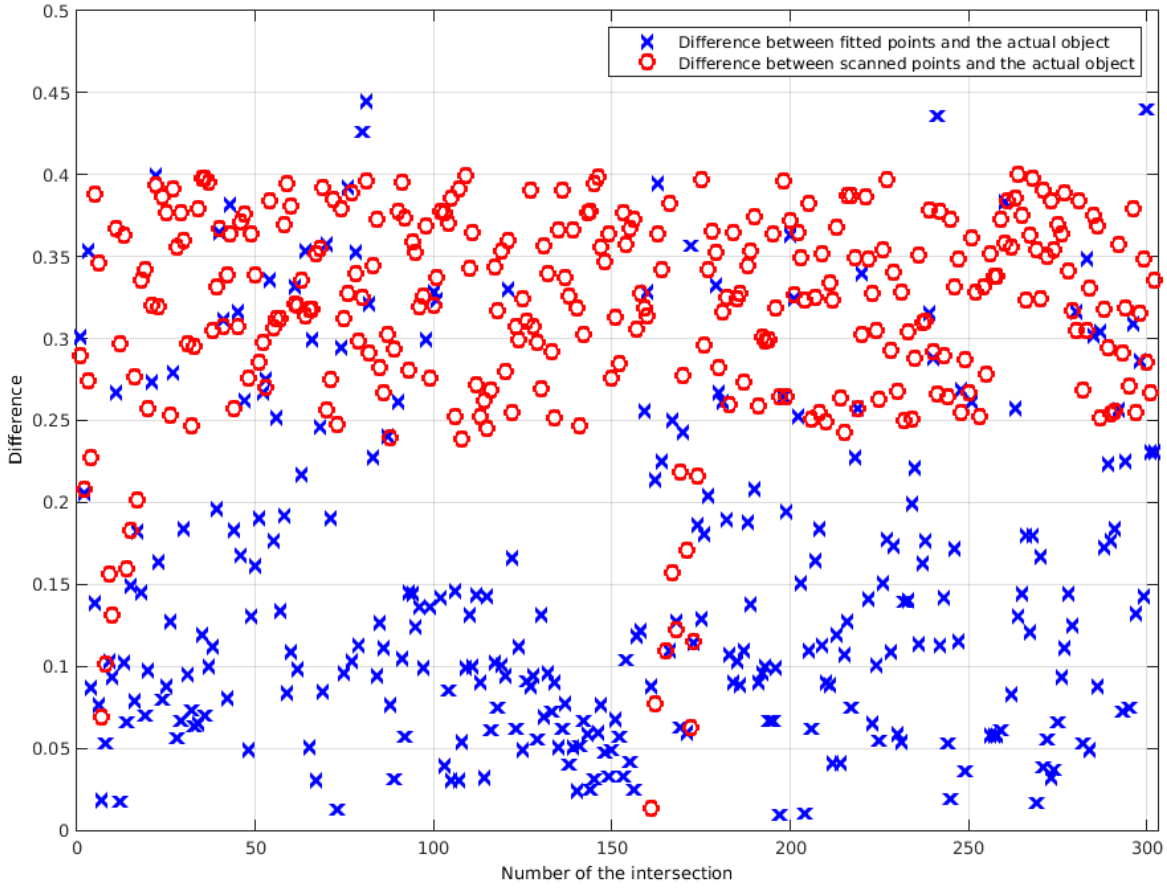

Figure 3.10: This figure shows the difference between the scanned points and the actual points of the object in Fig. 3.8. It also shows how the fitting has decreased the error to an almost half value.

in this case, an intelligent comprehensive method that covers all the situations of different objects.

3.6 Conclusion

This work presents our recently developed comprehensive and adaptive local scanning algorithms and method for fast scanning indiscrete objects. One important feature is that no prior information or preparing stages are required for our scanning method. Instead of a traditional raster scanning for searching the object in the scanning area, the effective initial search patterns are investigated. An effective initial search pattern, Start-6, is found and selected from many other common patterns based on extensive simulations and the efficiency factor. A sinusoidal scanning pattern is then used to scan the object and the frequency and amplitude of this sine wave would be adaptively adjusted based on predicting the curvature of the object. An Archimedean spiral search pattern is also used for missed points during the local scanning. In addition, the developed algorithms can find intersections and bifurcations on the object, and then resume the scanning from these points. To guarantee a comprehensive and intelligent scanning for any one-piece connected object, the developed algorithms consist of "double scanning prevention", "determining the side of a curve" and "returning from a lost tracking" as well. To minimize the object scanning error, a Fourier curve fitting is employed to improve the scanning accuracy. Extensive implementation results demonstrate that the fitting can reduce the scanning error to an almost half value. It also validates that our comprehensive and adaptive local scanning method can shorten the scanning time in order of hundreds of times in comparison to the traditional raster scanning without losing any important information about the scanned object.

Chapter 4

Accelerated Adaptive Local Scanning of Complicated Micro Objects for the PSD Scanning Microscopy: Methods and Implementation

4.1 Abstract

A PSD (Position Sensitive Detector) -based microscopy was introduced previously by same authors to scan sophisticated objects using the PSD sensor and a laser beam connected to an X-Y table [16, 19]. The system has numerous capabilities including but not limited to tracing an unknown object on the PSD, finding the dimensions of the object and adaptive local scanning for objects with intersections and bifurcations. Although promising results were obtained from that system, the speed of the scanning was still dependent on the speed of the movement of the micromanipulator. This work presents an extension to the tracing method and also introduces a completely novel system to eliminate the limitations of the micromanipulator. The simulations show a very fast scanning that does not need a laser and can scan the whole area of the PSD in a very short time.

Keywords - local scanning, adaptive method, complicated objects, scanning patterns, microscopy, quad-tree, 2D bisection

4.2 Introduction

In the previous works [16, 19], we developed a comprehensive and adaptive local scanning algorithm that is capable of rapidly scanning indiscrete, one-piece objects with various shapes such as open or closed curves, loops, intersections or bifurcations and so on. That proposed method does not require any prior information about the scanned objects nor does it need any preparation step. Instead, all the points are scanned on-line during the scanning. It uses an effective initial search pattern, Start-6, until one point of the object is found and then maps a sinusoidal scanning pattern to scan the object and the frequency and amplitude of this sine wave would be adaptively adjusted based on predicting the curvature of the object. An Archimedean spiral search pattern is also used for missed scanning. In addition, the developed algorithms can find intersections and bifurcations on the object, and then resume the scanning from these points. To minimize the object scanning error, a Fourier curve fitting was employed to improve the scanning accuracy. Extensive implementation results demonstrated that the fitting was able to reduce the scanning error to almost half. It also validated that our comprehensive and adaptive local scanning method can shorten the scanning time in order of hundreds of times in comparison to the traditional raster scanning without losing any important information about the object.

In this work, we first focused on objects with more complicated bifurcations. Namely, objects that have many branches and do not necessarily have any closed loop. These tree-shaped objects can be seen in branches of vein anatomy, dendrites and axon terminals of neurons and many other similar shapes.

Scanning these tree-shaped objects requires an intelligent algorithm that differentiates between the base and the branches from each other and is able to find and follow the correct path to scan the whole object. This was achieved by using a stack-based algorithm that maps the objects as it goes through it. Although promising results were obtained from this, but there would still be some cases that would have a missed branch due to the high angle of the path between a base and a branch. To be sure

that these problems are addressed, a Logarithmic spiral search is initiated after the algorithm finishes its normal scanning. This final scan would start from the center of the scanned object and would eventually find any missed branches.

The second part of this work tries to mitigate the problem of the speed of the X-Y table. Since the laser is required to move to scan the PSD area, the scanning speed would be directly dependent on the speed of the movement of the micromanipulator. No matter how much we increase the speed of the motors, there would still be this problem of moving the laser beam from one side to another. To address this problem, a novel idea was employed. In this new setup, a projector, focused on the PSD, would act like the laser beam and would give illumination on any points at any time. Since the only delay would be the refresh rate of the projector, which is in the scale of kilohertz, the scanning point can jump to any position in a time that is much faster than what PSD can capture. A Digital Light Processing (DLP) was used to give the best performance as the projector.

With having this ultra-fast solution available and based on the characteristics of the PSD sensor, we developed a new algorithm similar to the Quadtree method which in fact would follow a 2D bisection algorithm to find the object very quickly. This approach is to substitute the initial scanning that we had before. This would increase the scanning time significantly since the only limitation in time would be the response time of the PSD.

This paper is structured into the following sections: In Section 4.3, the scanning method for the tree-shaped object is introduced and the simulation results of the scanning would be presented. In Section 4.4, the 2D bisection method would be defined and the algorithm would be explained. Section 4.5 presents the results of the simulation of the 2D bisection method. Section 4.6 shows some of the filtering methods we used to get the best signal from the PSD. In Section 4.7 we conclude the work.

4.3 Scanning Tree-Shaped Objects

The scanning of the tree-shaped object needs an especial algorithm since the scanning pattern can get so complicated that might miss a considerable portion of the object. This can be seen in Fig. 4.1.

At first, we applied a few modifications to the section of the algorithm that detects and marks the bifurcations. By this, there would be much fewer chances of missing a branch but it still does not guarantee a definite fail-proof solution.

The challenge here is that since there is no prior information of the object, there might be cases that the branch is exactly perpendicular to the base. In such a scenario, a sinusoidal scanning pattern has a fifty percent chance of catching the branch. If the scanning pattern does not meet the branch, there would be absolutely no solution to extract that information later from the data.

A couple of methods was examined to prevent this problem. One approach might be to scan the whole object with a very low frequency sine wave after finishing the normal scanning. This can be very quick and also can reduce the possibility of missing a branch significantly.

Another solution would be to do a complete go-around search after finishing the scanning. In this approach, a scanning line would simply go around the object trying to constrain it in the smallest area that is possible. Since a not-scanned branch would be out of this border, it guarantees to not miss any branches. The problem with this method is that it is very hard to implement and verify.

The final approach is to add a final spiral search and continue the scanning from the newly founded points. This method is very fast and also easy to implement but it can introduce one serious challenge where the final spiral scan might find a branch that includes bifurcations itself. In another word, the new branch might be connected to a whole new group of branches that were not scanned before and therefore a missed branch would be a possibility after going through that group.

To address this problem the spiral search would continue until it exceeds the

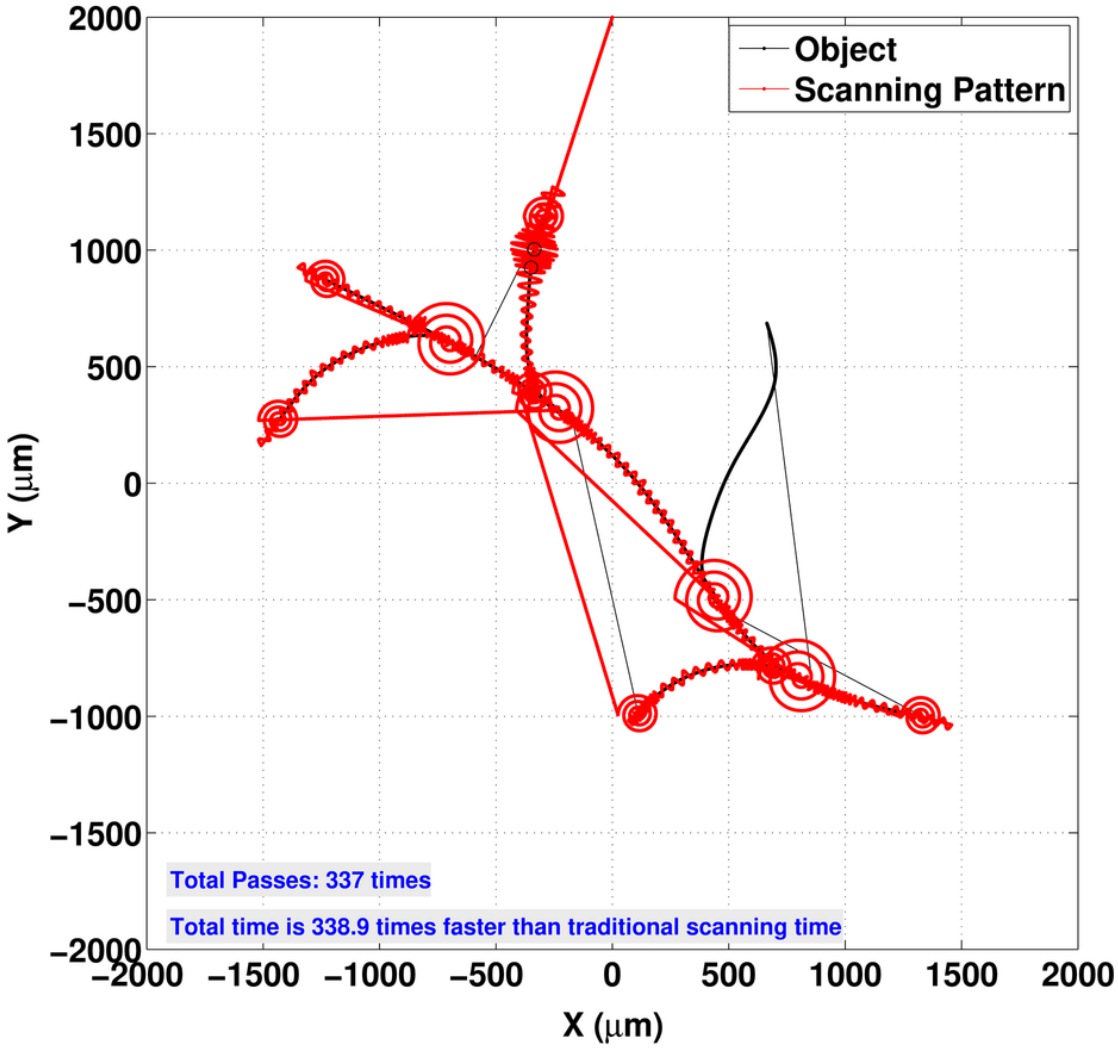

Figure 4.1: An unsuccessful scan is shown here. Color black represents the object and red is the scanning pattern.

furthest recognized point of the object.

To define a spiral search, two options were available. One to use an Archimedean spiral and the other to use a Logarithmic spiral. Fig. 4.2 shows the final Archimedean spiral scanning that is used with the same object as in Fig. 4.1.

A Logarithmic spiral can be defined in polar coordinates (r, θ) as:

$$\theta = \frac{1}{b} \ln \left(\frac{r}{a}\right) \tag{4.1}$$

With e being the base of natural logarithm, a and b being arbitrary positive real constants.

In parametric form, the curve is defined as:

$$\begin{aligned} x(t) &= r(t) \cos(t) = ae^{bt} \cos(t) \\ y(t) &= r(t) \sin(t) = ae^{bt} \sin(t) \end{aligned} \tag{4.2}$$

With real numbers a and b which would define the shape of the spiral.

To evaluate which spiral is more suitable for this specific situation, a simulation program was designed in MATLAB® and ran with many different objects. The results show some improvements in some cases and almost the same results in other cases. A small sample of these results are presented in Table 4.1. It should be noted that the simulation of others samples yielded almost same results as what is presented here.

Table 4.1: Comparison between different spirals scanning time

Sample	Scanning time with Archimedean spiral (s)	Scanning time with Logarithmic spiral (s)	Improvement (%)
First sample	142	131	7.7%
Second sample	177	176	0.5%
Third sample	208	196	5.8%

It can be concluded that using a Logarithmic spiral would improve the scanning time for an average of almost 5% but its other advantages and disadvantages are not clear and to be discussed. It should be noted that the a and b parameters of the

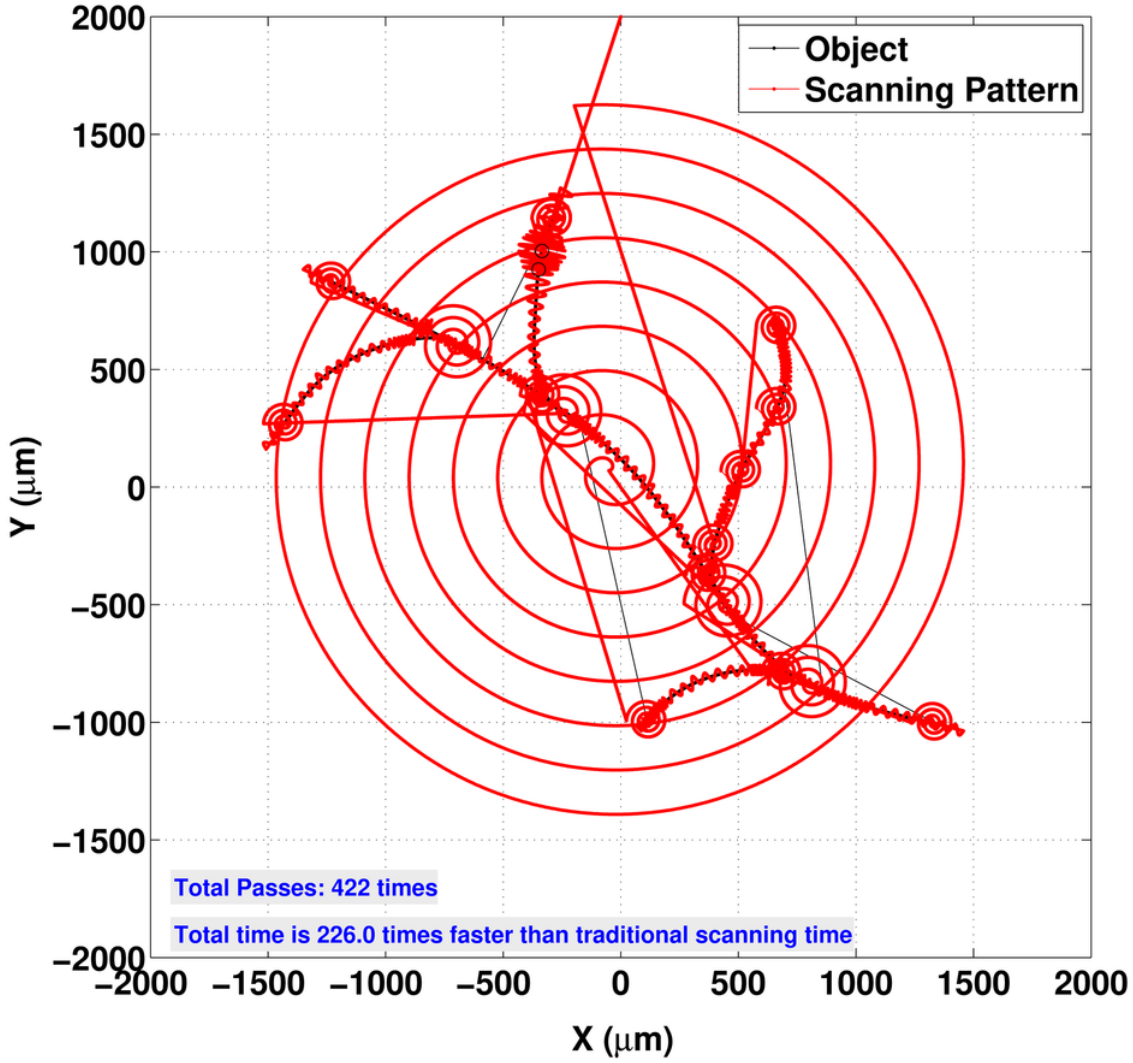

Figure 4.2: The same object as Fig. 4.1 but after all the modifications in the program and applying the final spiral search.

Logarithmic spiral have a significant impact on the shape of it. In these experiments $a = 50$ and $b = 0.07$ were selected by trial and error. Fig. 4.3 shows the Logarithmic spirals scanning of the same object that was used in Fig. 4.1.

Another example of a very complicated object and its final scanned result is presented in Fig. 4.4.

4.4 The 2D Bisection Method

This part of this work focuses on developing an accelerated adaptive local scanning method. This method can be used as the initial scanning to find the overall boundaries of the object. This method has a resemblance to the Quadtree method [20, 21] yet it is a completely different approach adopted for the PSD sensor. The principle though is more similar to a bisection method that is being used in a 2D space to locate the object on the PSD. This method works on fundamental behavior of the PSD sensor. A light spot presented on the active area will generate a photocurrent. The lateral-effect diodes are independent of the light spot profile and intensity distribution that affects the position reading in the segmented diodes. The input light beam may be of any size and shape since the position of the centroid of the light spot is indicated and provides electrical output signals proportional to the displacement from the center [1, 4, 2].

If we divide the area of the PSD into four equal sections and illuminate each whole section with a DLP projector, it can be understood if the object is covering any of that four sections. Since if the object is not covering a section, the resulted readout of the PSD would be the centroid of the section which would be the mathematical center of the section. But if the object is blocking a section, the readout of the PSD would be the centroid of the non-blocked portion of the section and would be definitely different than the mathematical center of the whole section. By comparing the readout of the PSD for each section with what we would expect if nothing had blocked that part, we can find out if the object is in that section or not. In another word, in each step, one section is chosen and a rectangular light is cast on that area. A comparison between the expected centroid position and the actual one would indicate if there is

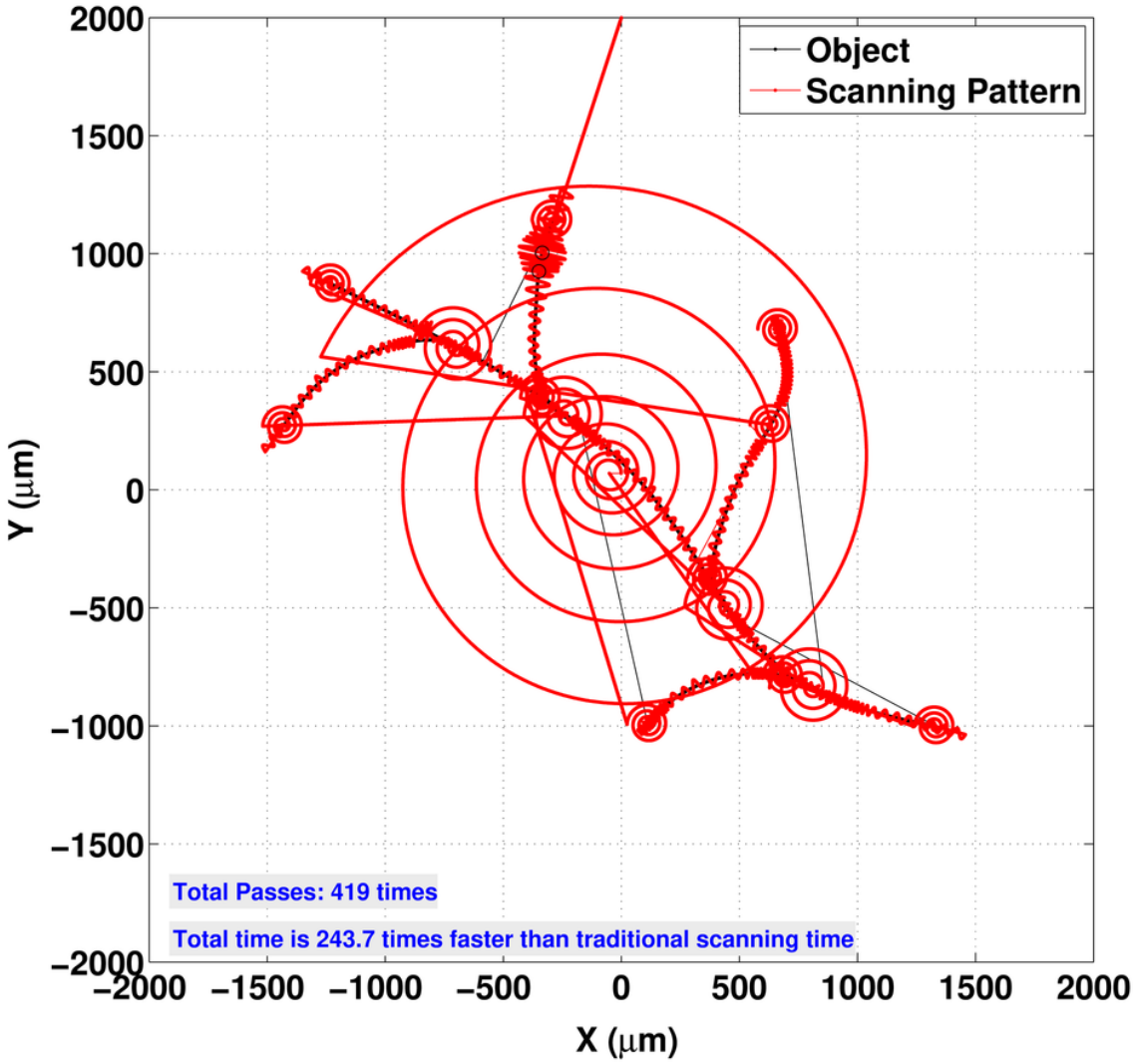

Figure 4.3: The same object as Fig. 4.1 is scanned with Logarithmic spiral pattern. The scanning time is improved by 7.7%

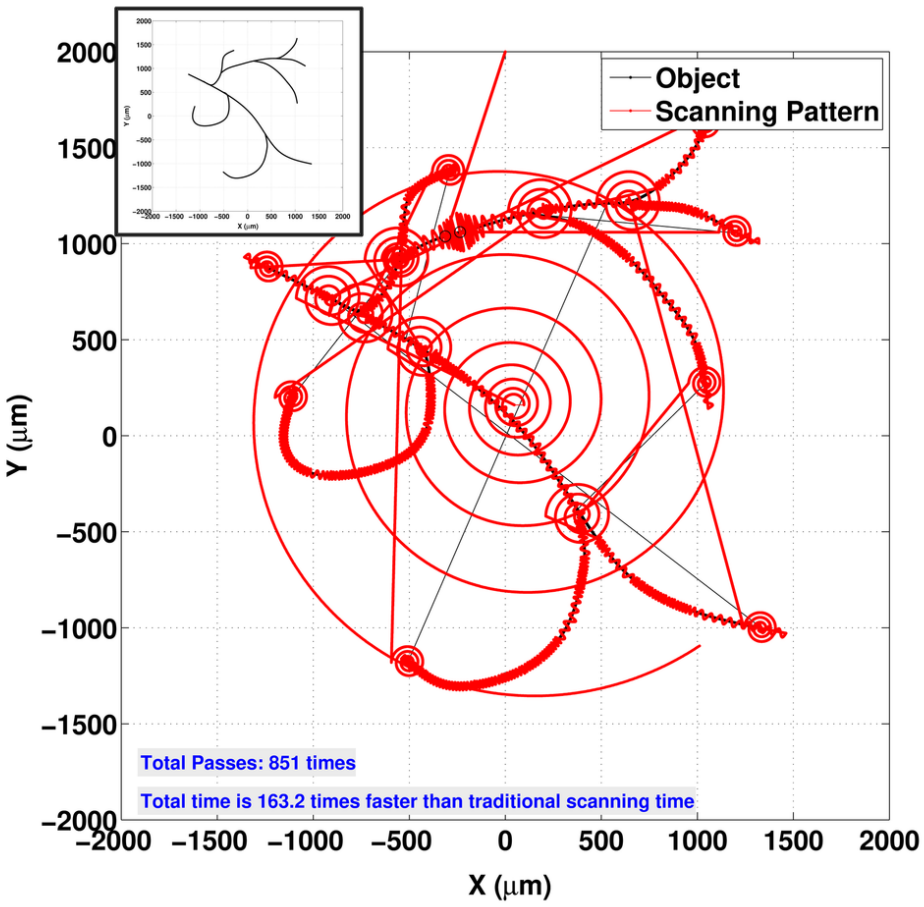

Figure 4.4: A very complicated sample is presented in the small box. The result of the scanning can be seen also.

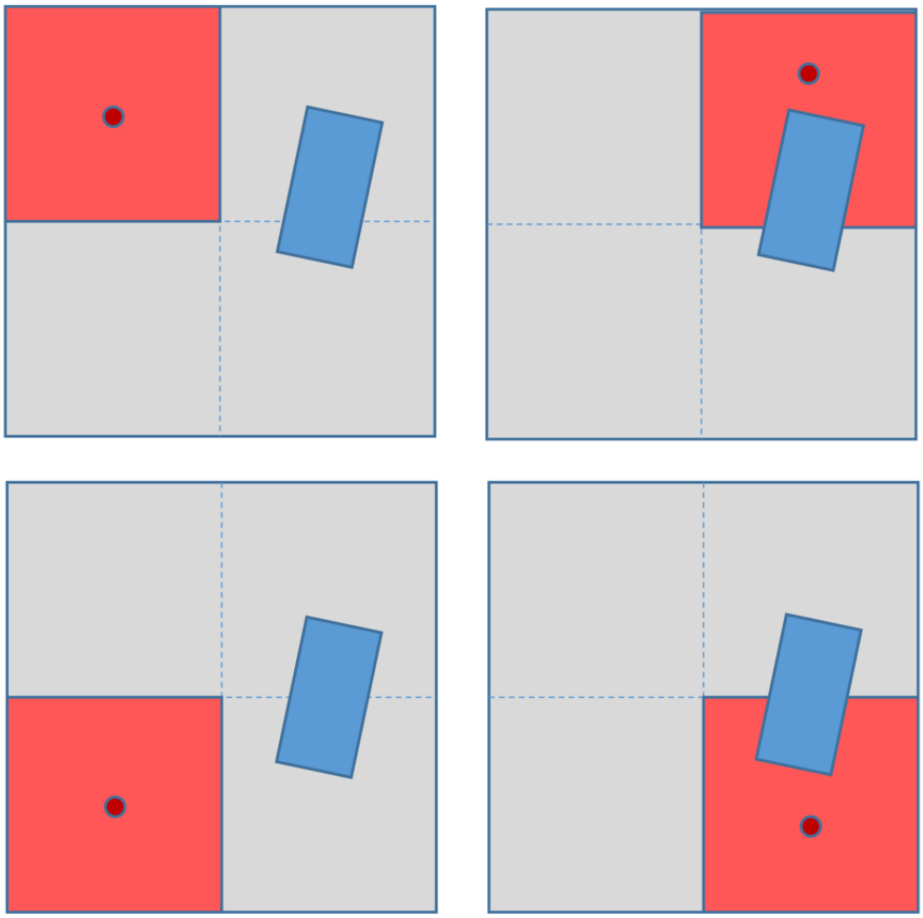

Figure 4.5: Four steps of the first scanning is presented. If the object is not blocking the illuminated section, the centroid point would be at the exact center but if it is blocking the light, the centroid point would be shifted toward the non-blocked portion of the section.

an object blocking the light in that area. This can be seen in Fig. 4.5. The next step is also shown in Fig. 4.6.

At this point, and by eliminating the sections that do not contain the object, we can further continue the algorithm to divide the sections that were partially blocked by the object into smaller sections and continue this until we either exactly map the object on the PSD or reach the response limitation of the PSD. Since we are dividing the whole area into the smaller parts we can reach one of those situations incredibly fast and also effectively.

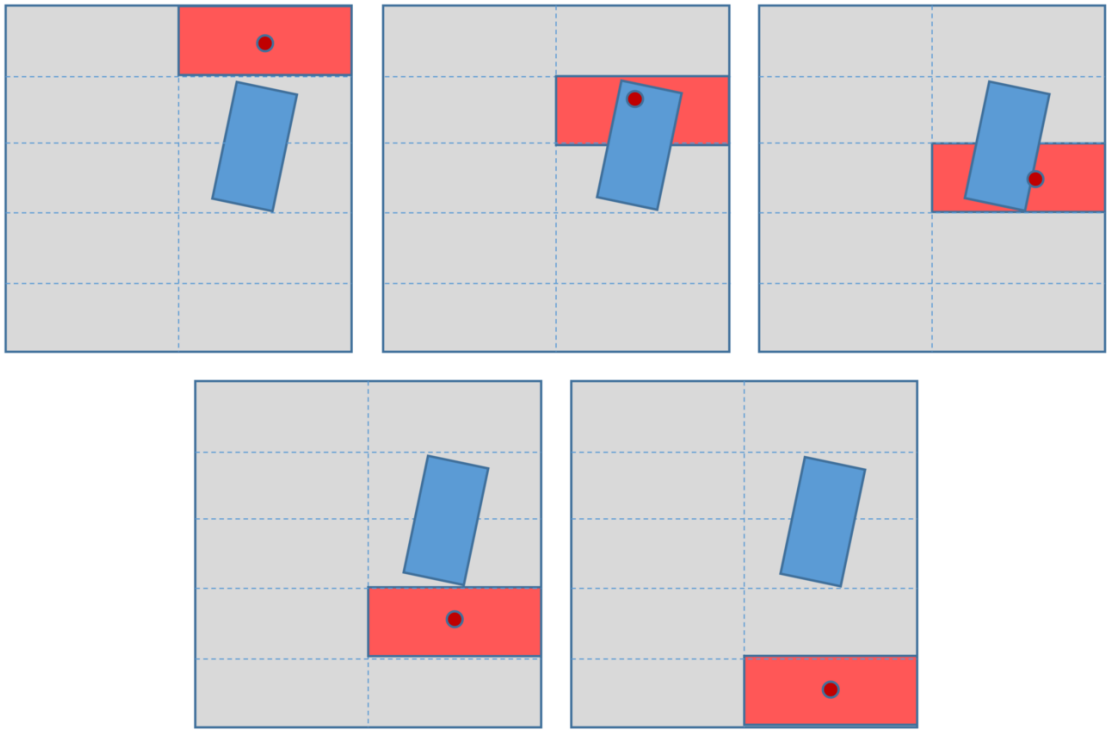

Figure 4.6: Six steps of the second scanning is presented here. For this specific object we can see that the program can easily eliminate three out of the six candidates that it got from the first scanning.

4.5 Simulation Of The 2D Bisection Method

A MATLAB simulation program was prepared to evaluate the effectiveness of the 2D bisection method. The input of the program is a given object and the program then follows the principles described in the previous section to perform the 2D bisection.

It is important to note that the process of performing the bisection cannot be continued indefinitely and has to be stopped at some point. For this system, that point would be defined by the physical properties of the PSD, the size of the PSD, the response of the signal acquisition system and the accuracy of the acquired signal. At some point and after following this bisection for a number of iterations, the displacement of the centroid of the illuminated area in comparison to the expected point would be insignificant. This can easily happen because of the section being too small and distinguishing between the displacement of the centroid and the noise being impossible. Considering the limits of the available PSD (a $4mm \times 4mm$ PSD) this limit was set as 6 iterations. Meaning that after finishing the bisection, the smallest section would be $(4^6)^{-1}$ or $\frac{1}{4096}$ of the whole area of the PSD.

The most important benefit of this method is eliminating the empty portions of the PSD by an exponential speed. This would result in reducing the scanning area significantly and therefore increasing the speed of the whole scan. An example of using this method is shown in Fig. 4.7. Considering this particular object, the result was achieved by the total of 109 scans which is the number of sections that were illuminated. For the final scanning of this object 57 of the smallest boxes would be needed. Since the smallest box is $\frac{1}{4096}$ of the whole area, therefore the final scanning area would be 0.0139 of the whole PSD.

This means that the scanning by using this method would be 72 times faster than scanning the whole area of the PSD since a significant portion of the PSD area is eliminated.

Another example is shown in Fig. 4.8. Note that although the object is positioned at the center of the PSD and hence should be involved in all the primary sections,

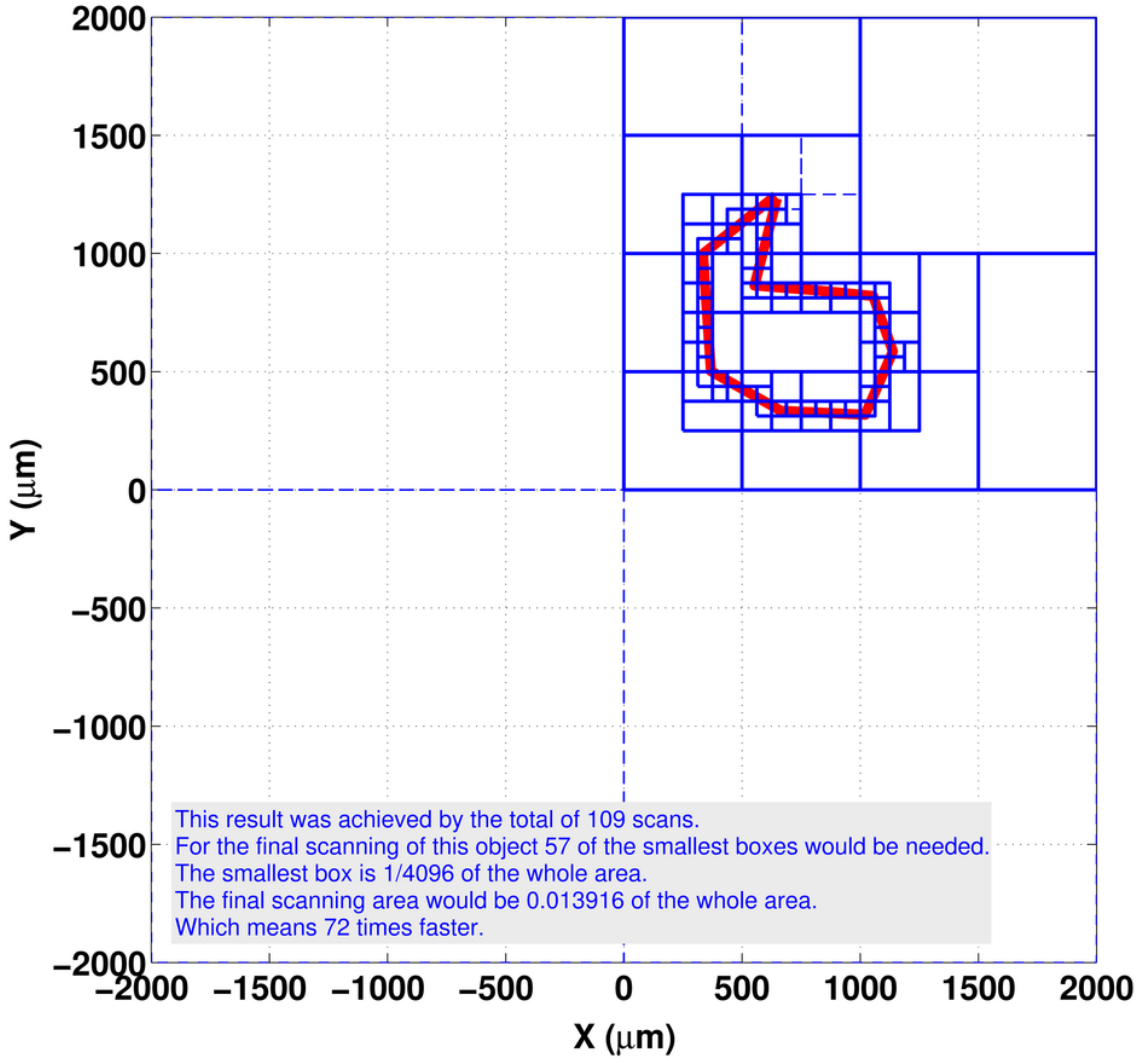

Figure 4.7: The result of using the 2D bisection method on a random sample is shown. Sample is presented in red color. Blue straight line are the sectioning of the program and the dashed lines are the sections that were eliminated.

because of continuing the method, we could still bound the object by smaller sections and as it can be seen, the result follows the previous example.

4.6 Filtering The PSD Output Noise

At this point, it is obvious that the accuracy of this method is directly dependent on the accuracy and trustworthiness of the signal that we get from the PSD. The smallest noise in the acquired signal can easily result in a big mistake in choosing the right section that is being covered by the object.

To filter the noise as much as we can, we used a three-step circuit. In the first step, we converted the output photocurrent of the PSD to the voltage. Then we used an amplifier circuit to change the range of the signal from 0 *to* 0.5 to -10 *to* 10 volts. The circuit can be seen in Fig. 4.9.

At the end, we used a double pole or 2^{nd} order low-pass Sallen-Key filter [22] to get the best signal to noise ratio. The 2^{nd} order low-pass Sallen-Key filter is shown in Fig. 4.10.

The transfer function of this second-order unity-gain low-pass filter is:

$$H(s) = \frac{{\omega_0}^2}{s^2 + 2\alpha s + {\omega_0}^2} \tag{4.3}$$

Where the undamped natural frequency f_0, attenuation α, Q factor and damping ratio ζ are given by:

$$\omega_0 = \frac{1}{\sqrt{R_1 R_2 C_1 C_2}} \tag{4.4}$$

$$2\alpha = 2\zeta\omega_0 = \frac{\omega_0}{Q} = \frac{1}{C_1}\left(\frac{R_1 + R_2}{R_1 R_2}\right) \tag{4.5}$$

The frequency response of the filter can be seen in Fig. 4.11 on the next page.

By using all these amplifiers and filters together we managed to reach a very clean signal from the PSD. To do a practical examination of the signal, we designed a

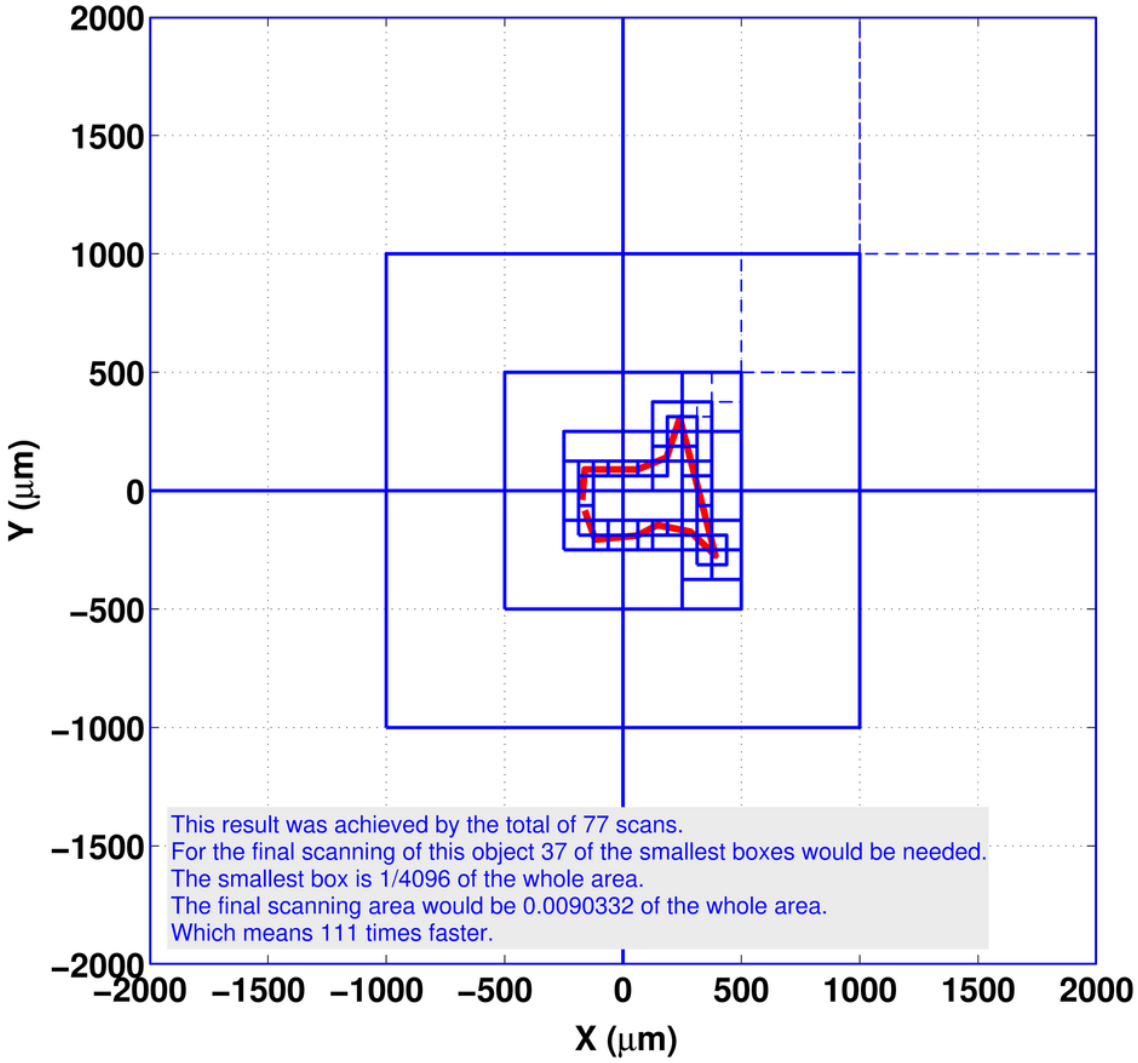

Figure 4.8: The result of using the 2D bisection method on a random sample located at the center of the PSD is shown here. Sample is presented in red color. Blue straight line are the sectioning of the program and the dashed lines are the sections that were eliminated. This result was achieved by a total of 77 scans. For the final scanning of this object 37 of the smallest boxes would be needed. The smallest box is 1/4096 of the whole area. The final scanning area would be 0.0090 of the whole PSD. Which means 111 times decrease in scanning time.

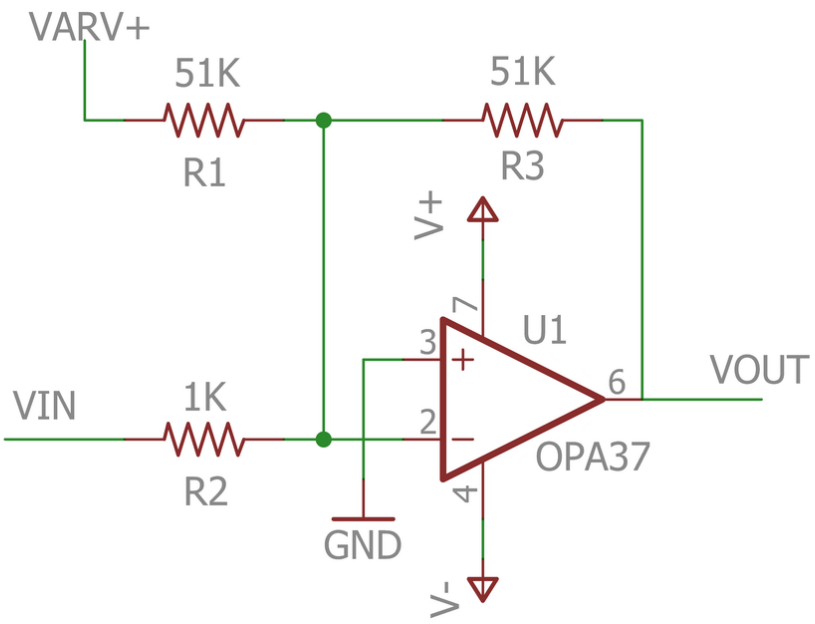

Figure 4.9: The amplifier circuit used to change the range of the input voltage.

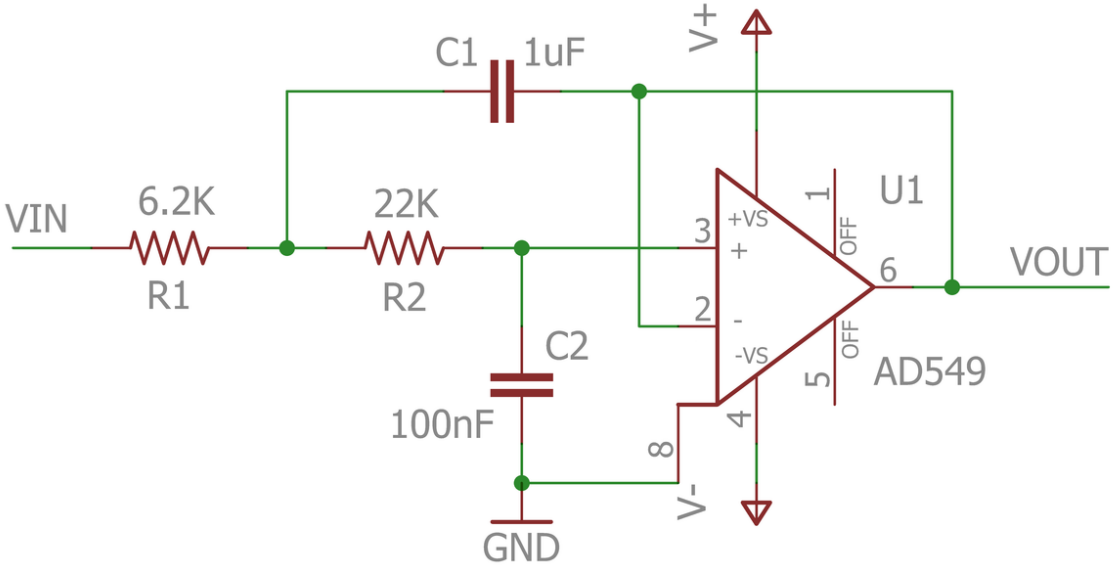

Figure 4.10: The low-pass Sallen-Key filter is used for filtering the noise before sending the signal to the DAQ.

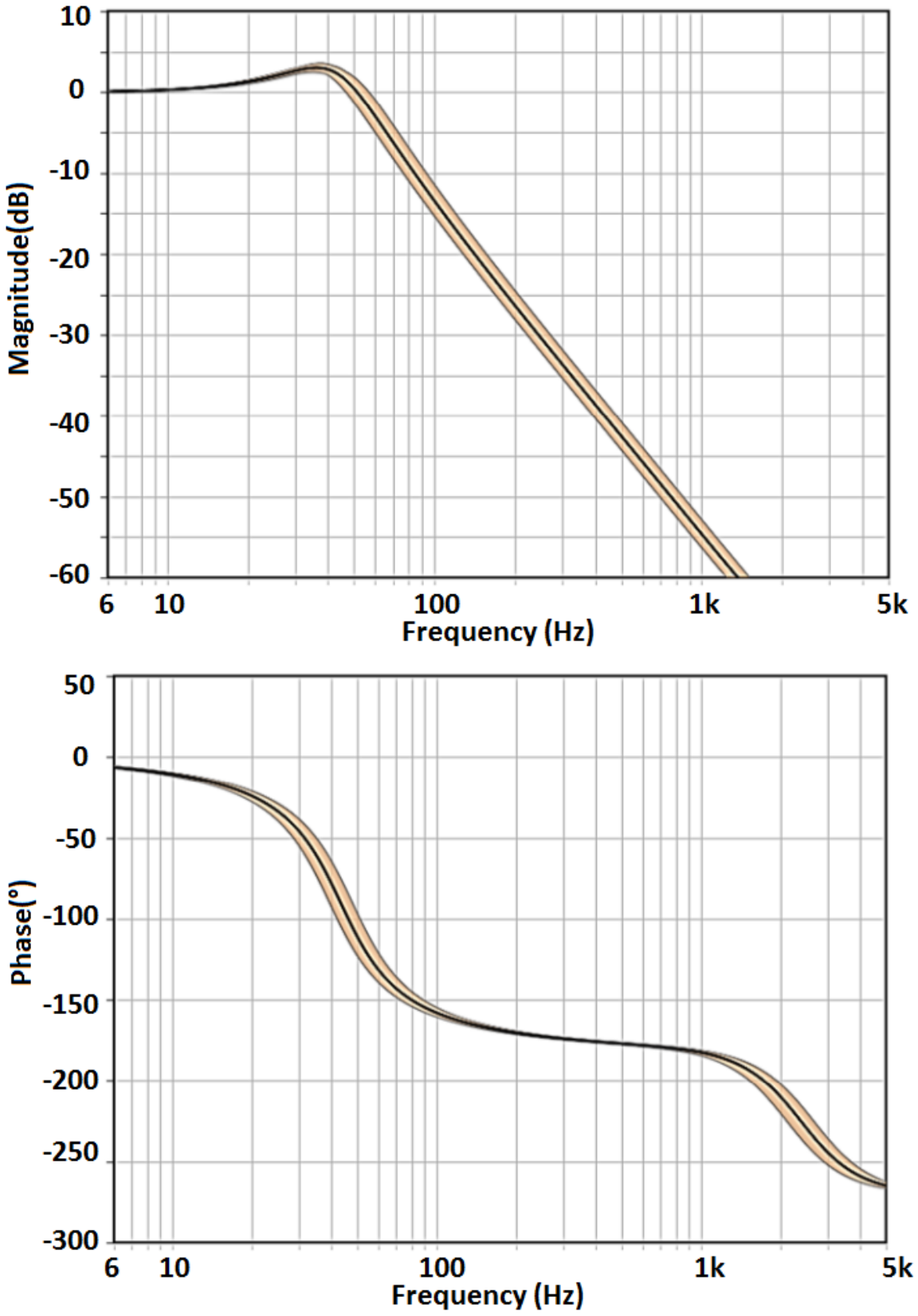

Figure 4.11: The frequency response of the low-pass Sallen-Key filter used. The value of the resistors and capacitors that resulted in this response can be seen in Fig. 2.5.

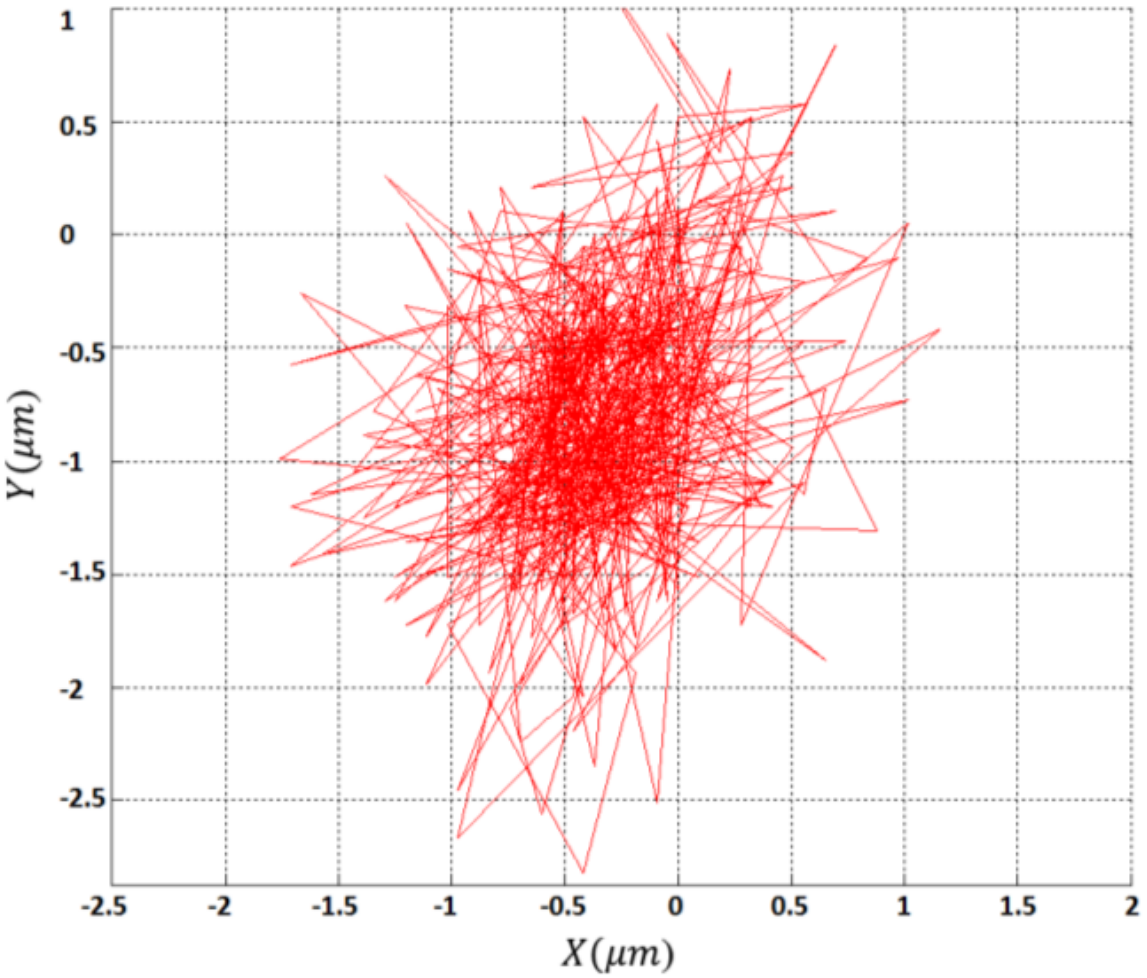

Figure 4.12: The effect of the noise when the laser is fixed is about $2\mu m$ is each direction.

simple test. We placed a laser on top of the PSD and without moving the laser we recorded the PSD output.

Fig. 4.12 on the next page shows the output of this experiment. As it can be seen, the effect of the noise of the reading of the PSD can be interpreted as a movement of about $2\mu m$ in each direction. Considering that this experiment was ran on a PSD with a size of $4mm \times 4mm$ we can conclude that the effect of the noise is 0.00003125% of the whole PSD since the area of the PSD is $16,000,000\mu m^2$ and the error is $5\mu m^2$. We think this is the best signal that can be extracted from the PSD.

By using a clean signal like this from the PSD we can make sure that our previously

implemented system is working fine.

4.7 Conclusion

This work presents our recent improvements of the PSD Microscopy. In the first part, we extended the work to scan tree-shaped objects. To achieve that we improved the algorithm and also introduced a final spiral search to find any missed branches. A comparison between Archimedean and Logarithmic spiral was also done to make sure which one is more suitable for this particular problem. At the end, we chose the Logarithmic spiral because of the slight improvement in the scanning time that it presents.

In the next part of the work, we introduced a 2D bisection method. Since we used a DLP projector instead of the laser beam we were able to illuminate some portions of the PSD. By using the characteristics of the PSD we developed the 2D bisection method.

The goal of it is to scan the whole area of the PSD very fact and in a few iterations. Although this method cannot find the exact dimensions of the object, what it can do is do eliminate some portions of the PSD area that does not include the object. In another word, in each iteration, some parts of the PSD is considered as not important for the scanning. After a few iterations, we can bound the object in a small box surrounding it and effectively reduce the final scanning area from the whole PSD to a small box that is around the object. By using this we can reduce the scanning time significantly. The simulation program that was created based on this method showed a reduction in scanning time in the scale of a couple order of magnitude.

We were also interested in getting a better signal out of the PSD and for this purpose we developed a circuit consisting of different steps of amplifying and filtering for each channel of the PSD.

We used a second-order low-pass Sallen-Key filter to clean out the noise that we were facing and after the implementation and testing, it was clear that the filtering is giving out a very suitable and clean signal. This filtering helps us to set better

decision points for the 2D bisection method.

In this work, we improved the previously introduced PSD microscopy by different approaches. This work can be further extended by examining the accuracy of the DLP projector and substituting the laser beam altogether. This requires a very suitable lens that maps the output of the DLP exactly on the PSD surface. Fine controlling of the DLP projector is another concern and needs more work.

By addressing these challenges in future, we can proceed to get more experimental results by using the PSD Microscopy.

Chapter 5

Conclusions and Future Work

5.1 Conclusion

In this study, we proposed a new microscopy system based on the PSD sensor and also developed and implemented the necessary methods and algorithm to do the scanning in time efficient manner and with good accuracy.

First, we improved the accuracy of the PSD sensor by minimizing the noises and distortions that were affecting the PSD. This was done by analyzing the noises and trying to eliminate them by various filters. We also used a rectifying method to mitigate the PSD distortion. Correction was made for X-Y mismatches and rotations and other affecting parameters. At the end, a microscopy system was proposed based on the improved PSD. Various experiments were performed to validate the accuracy of the system. A number of methods were also developed to scan solid or transparent objects. It became obvious that the system is capable of measuring the dimension of a small object with a very high accuracy and an error smaller than 2% in the whole scanning area.

The next step was to develop and implement an effective and efficient scanning method to decrease the scanning time of the area of the PSD. An adaptive local scanning method was developed to minimizing the time needed for this scanning. This is done by first using an initial scanning which would roughly find the position of the object and then a fine scanning that uses a sinusoidal pattern to scan the boundaries of the object. The pattern would follow the curvature of the object and

would even recognize bifurcations and crossings. This smart algorithm would change the amplitude and frequency of the sine wave automatically to match the circumstances of the object. Thick objects can also be scanned by using another smart method. Finally, a Fourier curve fitting is employed to get even better results from the reading we got from the scanning pattern. After doing numerous experiments it became clear that our comprehensive and adaptive local scanning method can shorten the scanning time in order of hundreds of times in comparison to the traditional raster scanning without losing any important information about the scanned object. This is due to the intelligent algorithm that can scan any object starting from any point of it.

The final section of this study was to go beyond the normal limitations and usage of the PSD. In this part, instead of using a single point light of the laser, a novel idea was employed. In this new setup, a projector, focused on the PSD, would act like the laser beam and would give illumination on any points at any time. Since the only delay would be the refresh rate of the projector, which is in the scale of kilohertz, the scanning point can jump to any position in a time that is much faster than what PSD can capture. By using this method, we developed a new technique that is similar to Quadtree and uses a 2D bisection algorithm to find the object very quickly.

The final result of this study is a new microscopy system that would use the PSD sensor to scan small objects. This system can scan an object as small as a few micrometers with very high accuracy and precision.

5.2 Future Work

The presented study shows the first steps toward the eventual implementation of a robust system approach for a new microscopy system. Although we have developed and implemented most of the algorithm and methods that are needed for this system, there are still improvements that can be done. All the current algorithm are written in MATLAB and need to be ported to C or C++ for using in an embedded micro-controller. By doing this, the system can be a stand-alone solution and would not need a computer to operate. Furthermore, improvements can be done in regard to

the DLP system and by using a DLP with higher resolution and response time we might get better results on the PSD. At the end, the proposed method can benefit from more experiments to find any problem that might be left. I hope this system would one day lead to a very cheap and accessible microscopy system that can benefit individuals and might be used in any lab or classroom.

References

[1] Hamamatsu Selection Guide, Solid State Division. *PSD (Position Sensitive Detectors)*, 2008. Hamamatsu.

[2] OSI Optoelectronics, webpage: www.osioptoelectronics.com. *PSD Characteristics*. Technical Statement.

[3] Helmuth Spieler. Introduction to radiation detectors and electronics. *VI. Position-Sensitive Detectors*, 1998.

[4] OSI Optoelectronics, webpage: www.osioptoelectronics.com. *Duo-Lateral, Super Linear PSD's*. page 48.

[5] Umer Hassan and Muhammad Sabieh Anwar. Reducing noise by repetition: introduction to signal averaging. *European Journal of Physics*, 31(3):453, 2010.

[6] Duane C Brown. Decentering distortion of lenses. *Photometric Engineering*, 32(3):444–462, 1966.

[7] Jason P De Villiers, F Wilhelm Leuschner, and Ronelle Geldenhuys. Centi-pixel accurate real-time inverse distortion correction. In *International Symposium on Optomechatronic Technologies*, pages 726611–726611. International Society for Optics and Photonics, 2008.

[8] Srinivasa M Salapaka and Murti V Salapaka. Scanning probe microscopy. *Control Systems, IEEE*, 28(2):65–83, 2008.

[9] Toshio Ando, Takayuki Uchihashi, Noriyuki Kodera, Daisuke Yamamoto, Atsushi Miyagi, Masaaki Taniguchi, and Hayato Yamashita. High-speed afm and nano-visualization of biomolecular processes. *Pflügers Archiv-European Journal of Physiology*, 456(1):211–225, 2008.

[10] Georg Schitter, Karl J Åström, Barry E DeMartini, Philipp J Thurner, Kimberly L Turner, and Paul K Hansma. Design and modeling of a high-speed afm-scanner. *Control Systems Technology, IEEE Transactions on*, 15(5):906–915, 2007.

[11] ADL Humphris, MJ Miles, and JK Hobbs. A mechanical microscope: high-speed atomic force microscopy. *Applied physics letters*, 86(3):34106–34106, 2005.

[12] YK Yong, SOR Moheimani, and IR Petersen. High-speed cycloid-scan atomic force microscopy. *Nanotechnology*, 21(36):365503, 2010.

[13] Peter I Chang and Sean B Andersson. A maximum-likelihood detection scheme for rapid imaging of string-like samples in atomic force microscopy. In *Decision and Control, 2009 held jointly with the 2009 28th Chinese Control Conference. CDC/CCC 2009. Proceedings of the 48th IEEE Conference on*, pages 8290–8295. IEEE, 2009.

[14] Peter I Chang and Sean B Andersson. Smooth trajectories for imaging string-like samples in afm: A preliminary study. In *American Control Conference, 2008*, pages 3207–3212. IEEE, 2008.

[15] Peter I Chang, Peng Huang, Jungyeoul Maeng, and Sean B Andersson. Local raster scanning for high-speed imaging of biopolymers in atomic force microscopy. *Review of scientific instruments*, 82(6):063703, 2011.

[16] Mehdi Rahimi, Yudong Luo, Frederick C Harris, Sergiu M Dascalu, and Yantao Shen. Improving measurement accuracy of position sensitive detector (psd) for a new scanning psd microscopy system. In *Robotics and Biomimetics (ROBIO), 2014 IEEE International Conference on*, pages 1685–1690. IEEE, 2014.

[17] Attila Kovács. Scanning strategies for imaging arrays. In *SPIE Astronomical Telescopes+ Instrumentation*, pages 702007–702007. International Society for Optics and Photonics, 2008.

[18] Kevin D Young. The selective value of bacterial shape. *Microbiology and molecular biology reviews*, 70(3):660–703, 2006.

[19] Mehdi Rahimi and Yantao Shen. Adaptive local scanning: A comprehensive and intelligent method for fast scanning of indiscrete objects. In *Intelligent Robots and Systems (IROS), 2015 IEEE/RSJ International Conference on*, pages 4955–4960. IEEE, 2015.

[20] Raphael A. Finkel and Jon Louis Bentley. Quad trees a data structure for retrieval on composite keys. *Acta informatica*, 4(1):1–9, 1974.

[21] Hanan Samet. The quadtree and related hierarchical data structures. *ACM Computing Surveys (CSUR)*, 16(2):187–260, 1984.

[22] Roy Pines Sallen and Edwin L Key. A practical method of designing rc active filters. *Circuit Theory, IRE Transactions on*, 2(1):74–85, 1955.